Melanophilin mediates the association of myosin-5a with melanosome via three distinct interactions

Jiabin Pan[‡§], Rui Zhou[‡§], Lin-Lin Yao[‡], Jie Zhang[‡], Ning Zhang[‡], Qin-Juan Cao[‡], Shaopeng Sun[‡§], and Xiang-dong Li[‡§1]

[‡]Group of Cell Motility and Muscle Contraction, State Key Laboratory of Integrated Management of Pest Insects and Rodents, Institute of Zoology, Chinese Academy of Sciences, Beijing 100101, China

[§]University of Chinese Academy of Sciences, Beijing 100049, China

[1]To whom correspondence should be addressed: Xiang-dong Li, Institute of Zoology, Chinese Academy of Sciences, Beijing 100101, China; Tel: +86-10-6480-6015; Email: lixd@ioz.ac.cn

Running title: Myosin-5a and melanophilin interaction

Key words: actin, melanophilin, melanosome, myosin-5a, Rab27a

ABSTRACT

Transport and localization of melanosome at the periphery region of melanocyte are depended on myosin-5a (Myo5a), which associates with melanosome by interacting with its adaptor protein melanophilin (Mlph). Mlph contains four functional regions, including Rab27a-binding domain, Myo5a GTD-binding motif (GTBM), Myo5a exon F-binding domain (EFBD), and actin-binding domain (ABD). The association of Myo5a with Mlph is known to be mediated by two specific interactions: the interaction between the exon-F-encoded region of Myo5a and Mlph-EFBD and that between Myo5a-GTD and Mlph-GTBM. Here, we identify a third interaction between Myo5a and Mlph, i.e., the interaction between the exon-G-encoded region of Myo5a and Mlph-ABD. The exon-G/ABD interaction is independent from the exon-F/EFBD interaction and is required for the association of Myo5a with melanosome. Moreover, we demonstrate that Mlph-ABD interacts with either the exon-G or actin filament, but cannot interact with both of them simultaneously. Based on above findings, we propose a new model for the Mlph-mediated Myo5a transportation of melanosomes.

Introduction

Melanosome is a specialized organelle within which melanin pigments are synthesized and stored. The peripheral accumulation of melanosomes in melanocytes is essential for the intercellular transfer of the organelles from the dendrite tips of melanocytes to the adjacent keratinocytes (Hume & Seabra, 2011). Microtubule and the associated motor proteins are responsible for the long-range and bidirectional transport of melanosomes between the nucleus to cell periphery, and actin filament and the associated motor protein myosin-5a (Myo5a) are essential for the short-distance transport and the capture of melanosomes at cell periphery (Wu et al., 1998; Wu & Hammer, 2014). The overall effect of the two transport systems is the peripheral accumulation of melanosomes in melanocytes. Lack of the latter causes the perinuclear accumulation of melanosomes in melanocytes, a phenotype called "dilute" (Provance et al., 1996; Wei et al., 1997).

Myo5a is a processive motor that has been implicated in the transportation and the tethering of organelles along actin filaments (Lindsay & McCaffrey, 2014; Mehta et al., 1999; Rudolf et al., 2011; Yoshimura et al., 2006; Zhang et al., 2018). Myo5a has two heavy chains, each containing an N-terminal motor domain, six IQ motifs that act as the binding sites for calmodulin (CaM) or CaM-like light chains, and a tail (Ikebe, 2008; Zhang et al., 2018). The tail of Myo5a can be further divided into three segments. The proximal tail is a long coiled-coil with length about 200 residues. The distal tail is the C-terminal globular tail domain (GTD). Between the proximal tail and the GTD is the middle tail, which is comprised of several short coiled-coils and the connecting loops. At least three essential functions are served by Myo5a tail. First, the coiled-coil regions enable Myo5a to form a dimer. Second, the GTD inhibits the motor activity of myosin head. Third, the tail is the binding site for the cargo proteins. The motor activity of Myo5a is tightly regulated (Krementsov et al., 2004; Li et al., 2006; Li et al., 2008; Li et al., 2004; Liu et al., 2006; Thirumurugan et al., 2006; Wang et al., 2004). In the inhibited state, Myo5a forms a folded conformation, in which the GTDs fold back to interact and inhibit the motor function. Upon being activated by high Ca^{2+}, cargo or adaptor proteins, Myo5a transforms from the folded conformation to the extended conformation, in which the GTD dissociates from the motor domain and the inhibition is relieved.

Melanophilin (Mlph) is one of the best-studied cargo proteins of Myo5a. Together with Rab27a, Mlph mediates the attachment of Myo5a to melanosomes. Rab27a is a small GTPase that, in the GTP-bound form, is anchored into the melanosome membrane via its lipid moiety (Ishida et al., 2014; Wandinger-Ness & Zerial, 2014) and Mlph bridges the interaction between Rab27a and Myo5a (Fukuda et al., 2002; Nagashima et al., 2002; X. S. Wu et al., 2002). The tripartite complex of Rab27a, Mlph, and Myo5a connects the melanosome to the actin filament. Lacking any one of these three components in melanocytes causes dilute phenotype (perinuclear accumulation of melanosomes) (Fukuda et al., 2002; Hume et al., 2001; Strom et al., 2002; Wei et al., 1997; Wu et al., 2001; X. S. Wu et al., 2002).

Mlph contains four functional regions, including RBD (Rab27a-binding domain), GTBM (Myo5a GTD-binding motif), EFBD (Myo5a exon F-binding domain), and ABD (actin-binding domain)(Fukuda et al., 2002; Geething & Spudich, 2007; Li et al., 2005; Yao et al., 2015). The association of Myo5a with Mlph involves two molecular interactions. One is the interaction between the exon-F-encoded region (exon-F for simplification) of Myo5a and the EFBD of Mlph (Fukuda & Itoh, 2004; X. Wu et al., 2002; X. S. Wu et al., 2002). Exon-F is an alternatively spliced exon presents in the middle tail of the melanocyte-spliced isoform of Myo5a (Huang et al., 1998). The exon-F/EFBD interaction is absolutely essential for the localization of Myo5a to the melanosome (X. Wu et al., 2002). The other interaction is between the GTD of Myo5a and the GTBM of Mlph (Geething & Spudich, 2007; Pylypenko et al., 2013; Wei et al., 2013). We previously found that GTBM activates Myo5a motor function by relieving the GTD inhibition on the motor domain and inducing a folded-to-extended conformational transition of Myo5a (Li et al., 2005; Yao et al., 2015). Recently, we demonstrated that the activation of Myo5a by Mlph-GTBM is regulated by another Myo5a-binding protein RILPL2 (Rab-interacting lysosomal protein-like 2) and the small GTPase Rab36, a binding partner of RILPL2 (Cao et al., 2019).

Mlph-ABD is essential to proper melanosome transport (Fukuda & Kuroda, 2002; T. S. Kuroda et al., 2003; Taruho S. Kuroda et al., 2003). Besides being able to bind to actin filament, Mlph-ABD could interact with end-binding protein 1, which might facilitate the transfer of melanosomes from microtubules to actin (Wu et al., 2005). *In vitro* motility assays at single-molecular level show that Mlph prolongs and slows the processive movements of Myo5a, presumably via the interaction between ABD and actin filament (Sckolnick et al., 2013). A cluster of conserved positively charged residues in ABD is essential for actin binding and Melanophilin localization in melanocytes (T. S. Kuroda et al., 2003). An *in vitro* study suggests that Mlph-ABD is a target of protein kinase A and that the phosphorylated Mlph preferred binding to actin even in the presence of microtubules, whereas dephosphorylated Mlph bind to microtubules (Oberhofer et al., 2017).

Biochemical analysis of Mlph show that the ABD is not essential for the interaction with Myo5a nor the activation of Myo5a motor function, suggesting that a truncated Mlph protein containing the RBD and the two Myo5a-binding domains (the GTBM and the EFBD) but lacking the ABD is able to form a tripartite complex with Rab27a and Myo5a and thus sufficient for the recruitment of Myo5a to melanosome membrane (T. S. Kuroda et al., 2003; X. Wu et al., 2002). However, using melan-ln cells (Mlph-null melanocytes), Hume et al. have found that the ABD-deleted Mlph cannot to promote the recruitment of Myo5a onto melanosomes, indicating that the ABD is necessary *in situ* for the association of Myo5a with Mlph (Hume, 2006). This discrepancy between *in vitro* and cell culture results promoted us to investigate the interaction between Mlph-ABD and Myo5a.

In this study, we have identified a third interaction between Myo5a and Mlph, i.e., the interaction between the exon-G-encoded region (exon-G for simplification) of Myo5a and Mlph-ABD. We find that the exon-G/ABD interaction is independent from the exon-F/EFBD interaction, and that, similar to exon-F/EFBD, exon-G/ABD is essential for the dilute-like phenotype induced by Myo5a-tail overexpression. Moreover, we demonstrate that Mlph-ABD interacts with either the exon-G of Myo5a or actin filament, but cannot interact with both of them simultaneously. Based on above findings, we propose a new model for the Mlph-mediated Myo5a transportation of melanosomes.

RESULTS

The actin-binding domain of melanophilin (Mlph-ABD) contains a novel Myo5a-binding site.

Myo5a binds to its cargo proteins, including Mlph, majorly via the middle tail domain (MTD, residues 1106-1467) and the GTD (residues 1468-1877) (Figure 1A, top). The C-terminal portion of the MTD is encoded by a serial exons, called exon-A to -G, among which exon-B, -D, and -F are alternatively spliced exons (Seperack et al., 1995). The melanocyte isoform of Myo5a contains exon-D and -F (Figure 1A, middle), whereas the brain isoform contains exon-B. The MTD is predicted to form four short coiled-coils, among which the last one is formed by the C-terminus of exon-F and the entire exon-G (Figure 1A, bottom).

To detect interaction between the ABD of Mlph with Myo5a, we performed GST pulldown assay using GST-Mlph-ABD (the GST-tagged ABD of Mlph, residues 401-590) and Flag-Myo5a-MTD (the Flag-tagged middle tail domain of Myo5a, residues 1106-1467) (Figure 1A and 1B). GST-Mlph-ABD was expressed in E. coli and purified by GSH-Sepharose chromatography, and Flag-Myo5a-MTD was expressed in Sf9 cells and purified by anti-Flag affinity chromatography. GST pulldown assay shows that GST-Mlph-ABD specifically interacted with Flag-Myo5a-MTD (Figure 1C, lane 2). Deleting the residues 401-437 of Mlph-ABD had little effect on the interaction with Myo5a-MTD (Figure 1C, lane 3 and 4), indicating the N-terminal 37 residues of Mlph-ABD are not essential for the interaction. Further deletion of 437-446 slightly decreased the interaction and deletion of 446-455 eliminated the interaction (Figure 1C, lane 5 and 6), indicating that residues 446-455 are essential for the interaction with Myo5a-MTD. Similarly, we performed C-terminal truncation analysis of Mlph-ABD on the interaction with Myo5a-MTD and identified residues 560-571 essential for the interaction (Figure 1D). Taking together, we identified the middle portion of Mlph-ABD (residues 446-571) as the core of the novel binding site for Myo5a-MTD.

We then produced a number of truncated Myo5a-MTD constructs and performed GST pulldown assays to narrow down the region in Myo5a-MTD binding to Mlph-ABD (Figure 2A). To simplify the experiments, we first compared the bacterial-expressed Myo5a-MTD with the Sf9 cell-expressed Myo5a-MTD in the interaction with Mlph-ABD. GST pulldown assay shows that both versions of Myo5a-MTD specifically interacted with Mlph-ABD (Figure 2-figure supplement A). All the following pulldown experiments were performed using the bacterial-expressed Myo5a-MTD, unless otherwise indicated. C-terminal truncation of Flag-Myo5a-MTD shows that the C-terminal half of exon-G (residues 1453-1467) is essential for binding to Mlph-ABD (Figure 2-figure supplement B). Mlph-ABD interacted strongly with Flag-Trx-Myo5a (1411-1467) (a short peptide containing exon-F and exon-G), but weakly with Flag-Trx-Myo5a (1436-1467) (a short peptide containing exon-G) (Figure 2-figure supplement C, lane 3 and 4), suggesting that exon-F might be required for strong interaction of exon-G with Mlph-ABD. However, deletion of exon-F from Myo5a-MTD did not affect the interaction with Mlph-ABD (Figure 2B, lane 2), indicating that exon-F is not essential for the interaction. Deletion of the C-terminal portion (residues 1454-1467) of exon-G abolished the binding of Myo5a-MTD with Mlph-ABD (figure 2B, lane 3), but did not affect the interaction of Myo5a-MTD with Mlph-EFBD (Figure 2C). Figure 2A summaries the truncation analysis of the interaction between Myo5a-MTD and Mlph-ABD. Based on above results, we conclude that the exon-G of Myo5a binds to Mlph-ABD.

Characterization of the exon-G/ABD interaction.

To characterize the exon-G/ABD interaction, we monitored the interaction between Myo5a-MTD and Mlph-ABD using microscale thermophoresis (MST), and obtained the dissociation constant (K_d) of 562±169 nM of Myo5a-MTD for binding to Mlph-ABD (Figure 3A). Consistent with the pulldown assay (Figure 2B), deletion of the C-terminal half of exon-G (Myo5a-MTDΔG) greatly decreased the MST signaling (Figure 3A). We then investigated the effect of ionic strength on the exon-G/ABD interaction. GST pulldown assays of GST-Mlph-ABD and Flag-Myo5a-MTD were conducted in the presence different concentrations of NaCl. Compared with 100 mM NaCl, 300 mM and 500 mM NaCl greatly decreased the

151 amount of Flag-Myo5a-MTD pulled down with GST-Mlph-ABD (Figure 3B), suggesting that ionic
152 interactions are critical for the exon-G/ABD interaction.

153 Sequence alignment among the Mlph of mammals and birds reveals several highly conserved charged
154 residues in the two regions of Mlph-ABD essential for the interaction with Myo5a-MTD, including four
155 acidic residues (D447, E449, E452, and E454) in the residues 446-455 and two basic residues (R562 and
156 R568) in the residues 560-571 (Figure 3C). To determine the roles of those conserved charged residues of
157 Mlph on the exon-G/ABD interaction, we mutated them individually into alanine. GST pulldown assays
158 show that both E449A and E452A mutations abolished the interaction with Myo5a-MTD, whereas other
159 mutations (D447A, E454A, R562A, R568A) had little effect on the interaction (Figure 3E), indicating that
160 both E449 and E452 of Mlph are essential for the exon-G/ABD interaction.

161 We expected the conserved acidic residues E449 and E452 of Mlph to interact with the conserved
162 basic residues in the exon-G of Myo5a. Sequence alignment of the three Myo5 isoforms of mammals and
163 birds reveals two highly conserved basic residues (K1456 and K1460) in the C-terminal portion of exon-G
164 of Myo5a (Figure 3D). GST pulldown assay shows that both K1456A and K1460A mutations substantially
165 decreased the amount of Flag-Myo5a-MTD pulled down with GST-Mlph-ABD (Figure 3F), suggesting that
166 both K1456 and K1460 of Myo5a play a key role in the interaction with Mlph-ABD.

167 **The exon-F/EFBD interaction and the exon-G/ABD interaction are independent from each other.**

168 Because exon-F and exon-G are in immediate vicinity, it is possible that the exon-F/EFBD interaction
169 and the exon-G/ABD interaction interfere with each other. To test this possibility, we performed GST
170 pulldown assays of GST-Mlph-ABD and Flag-Mlph-EFBD in the presence or absence of
171 Flag-Myo5a-MTD. If Myo5a-MTD is able to interact with both Mlph-ABD and Mlph-EFBD
172 simultaneously, a tripartite complex will be formed by Myo5a-MTD, Mlph-ABD, and Mlph-EFBD (Figure
173 4A, upper panel), and Flag-Mlph-EFBD will be pulled down with GST-Mlph-ABD in the presence of
174 Flag-Myo5a-MTD. As shown in Figure 4A, Flag-Mlph-EFBD was pulled down with GST-Mlph-ABD in
175 the presence of Flag-Myo5a-MTD, but not in the absence of Flag-Myo5a-MTD. This result is consistent
176 with a scenario that Myo5a-MTD binds to both Mlph-EFBD and Mlph-ABD simultaneously. We therefore
177 conclude that the exon-F/EFBD interaction and the exon-G/ABD interaction do not interfere with each
178 other.

179 As the exon-F/EFBD interaction and the exon-G/ABD interaction are independent to each other, we
180 expected that those two interactions act synergically for the binding of Myo5a-MTD to Mlph. As expected,
181 GST pulldown assays show that GST-Mlph-ΔRBD, which contains both EFBD and ABD, strongly bound
182 to Flag-Myo5a-MTD, and deletion of either exon-F or exon-G from Myo5a-MTD substantially weakened
183 the interaction with GST-Mlph-ΔRBD (Figure 4B). Conversely, Flag pulldown shows that substantial
184 amount of GST-Mlph-ΔRBD could be pulled down with Flag-Myo5a-MTD, and deleting ABD from
185 GST-Mlph-ΔRBD strongly decreased the amount of protein pulled down with Flag-Myo5a-MTD (Figure
186 4C). Above results indicate that the exon-F/EFBD interaction and the exon-G/ABD interaction act
187 synergically, resulting in a strong interaction between Myo5a-MTD and Mlph.

188 **Mlph-ABD cannot interact with F-actin and exon-G simultaneously.**

189 In addition to interacting with the exon-G of Myo5a, Mlph-ABD is able to bind to actin. To investigate
190 whether Mlph-ABD interacts with actin and exon-G simultaneously, we performed actin co-sedimentation
191 of Mlph-ABD and Myo5a-MTD. As expected, substantial amount of Mlph-ABD, but essentially no
192 Myo5a-MTD, was co-sedimentated with F-actin (Figure 5A). Interestingly, Mlph-ABD did not increase the
193 amount of Myo5a-MTD co-sedimentated with F-actin (Figure 5A), suggesting that Mlph-ABD cannot
194 interact with F-actin and exon-G simultaneously.

195 The inability of Mlph-ABD to interact with F-actin and exon-G simultaneously suggests that F-actin
196 and exon-G compete in binding to Mlph-ABD. It is possible that Myo5a-MTD might antagonize the
197 interaction between Mlph-ABD and F-actin. To test this possibility, we performed F-actin

198 co-sedimentations of Mlph-ABD in the presence of different concentrations of Myo5a-MTD. As expected,
199 Myo5a-MTD substantially decreased the amount of Mlph-ABD co-sedimentated with F-actin (Figure 5B).
200 We therefore concluded that Mlph-ABD cannot bind to F-actin and exon-G simultaneously and those two
201 interactions are mutually exclusive.

202 **The exon-G/ABD interaction is essential for Myo5a-tail to induce dilute-like phenotype in**
203 **melanocytes.**

204 Myo5a associates with melanosome via its interaction with Mlph, which attaches to melanosome via
205 the interaction between its RBD and the melanosome-bound Rab27a. Overexpression of the EGFP fusion
206 protein of Mlph-ΔRBD in the melanocyte cell line, melan-a, caused dilute-like phenotype, i.e., the
207 perinuclear distribution of melanosomes in melanocyte (Figure 6A, Figure 6-figure supplement).
208 Generation of dilute-like phenotype by Mlph-ΔRBD was attributed to the ability of Mlph-ΔRBD to compete
209 with the melanosome-bound Mlph in interacting with Myo5a molecules, thereby dissociating Myo5a from
210 melanosome. To investigate whether the exon-G/ABD interaction is essential for the dominant negative
211 effect of Mlph-ΔRBD in melanocyte, we introduced two single pointed mutations, E449A and E452A, in
212 Mlph-ΔRBD, both of which are essential for Mlph-ABD to interact with the exon-G (Figure 3E). We found
213 that both two mutations substantially decreased the number of the transfected cells with dilute-like
214 phenotype. While dilute-like phenotype was presented in 48.78% of cells expressing the wild-type
215 Mlph-ΔRBD, only in 20.97% and 19.07% of cells expressing E449A and E542A, respectively (Figure 6B).
216 Western blots of the lysate of transfected cells showed no degradation of the expressed proteins of
217 EGFP-Mlph-ΔRBD WT and two mutants (Figure 6C). Based on the band densities in the Western blot and
218 the transfection efficiencies of those three constructs, we estimated the relative protein expression levels of
219 each transfected cells for EGFP-Mlph-ΔRBD WT, E449A, and E452A were roughly equal (Figure 6C).
220 Therefore, we conclude that the inability of E449A and E452A mutants to generate dilute-like phenotypes
221 was not due to the intracellular degradation or the low expression level of the EGFP fusion proteins.

222 To further determine the role of the exon-G/ABD interaction on the tethering of Myo5a with Mlph in
223 melanocyte, we expressed the EGFP fusion protein of Myo5a-tail (residues 1106-1877), which contains all
224 three Mlph-binding regions, i.e., exon-F, exon-G, and GTD (Figure 7A). Overexpressing the tail region of
225 Myo5a in melanocyte was expected to compete with endogenous Myo5a in interacting with Mlph, thus
226 causing dilute-like phenotype (Wu et al 2002). Deletion analysis of the tail region of Myo5a have shown
227 that both exon-F and the GTD are required and that neither of them alone is sufficient for generating the
228 dominant negative phenotype in melanocytes (Wu et al 2002). Similar to the previous report, Myo5a-tail is
229 well co-localized with both melanosome and Mlph, and generated dilute-like phenotype in ~50% of
230 transfected melan-a melanocytes (Figure 7B and 7C). In contrast, Myo5a-TailΔG generated dilute-like
231 phenotype in only ~10% of transfected cells (Figure 7B and 7C, Figure 7-figure supplement). Western blot
232 of the lysate of transfected cells showed no degradation of the expressed proteins of EGFP-Myo5a-Tail WT
233 and ΔG (Figure 7D). Based on the band densities in the Western blot and the transfection efficiencies, we
234 estimated the relative protein expression levels of each transfected cells for EGFP-Myo5a-Tail WT and ΔG
235 were roughly equal. Therefore, we conclude that the inability of EGFP-Myo5a-Tail ΔG to generate
236 dilute-like phenotypes was not due to the intracellular degradation or the low expression level of the EGFP
237 fusion protein.

238 Based on above results, we concluded that, similar to exon-F, exon-G is also required for Myo5a-Tail
239 to disrupt endogenous Myo5a function in transportation of melanosomes.

240 **Myo5a-MTD colocalized with Mlph but was unable to induce dilute-like phenotype.**

241 Unlike Myo5a-Tail, overexpression of Myo5a-MTD, which contains both exon-F and exon-G but
242 lacks the GTD, did not generate dilute-like phenotype in melan-a cells. However, Myo5a-MTD is well
243 colocalized with endogenous Mlph and partially colocalized with melanosome (Figure 8A). We reasoned

that the presence of both exon-F and exon-G is insufficient for binding to the Mlph occupied by Myo5a, but sufficient for binding to the unoccupied Mlph.

Deletion of exon-F almost eliminated the co-localization of Myo5a-MTD and Mlph (Figure 8B), consistent with its essential role for the binding of Myo5a with Mlph. Deletion of exon-G substantially decreased, but did not eliminate, the co-localization of Myo5a-MTD and Mlph (Figure 8C), indicating that exon-G plays an auxiliary role for binding of Myo5a with Mlph.

DISCUSSION

It is well-established that Myo5a associates with melanosome via two independent interactions with Mlph, i.e., the interaction between exon-F of Myo5a and Mlph-EFBD and the interaction between the GTD and Mlph-GTBM. In the current study, we identified the third interaction between Myo5a and Mlph, i.e., the interaction between the exon-G of Myo5a and the Mlph-ABD. We demonstrated that, similar to the exon-F/EFBD interaction, the exon-G/ABD interaction is also required for the strong binding of Myo5a and Mlph.

Among the three interactions between Myo5a and Mlph, the GTD/GTBM interaction majorly regulates the motor function of Myo5a. At relative high ionic strength but not at physiological ionic strength, Mlph-GTBM binds to the GTD, inducing Myo5a to form the extended conformation and activating Myo5a motor activity (Li et al., 2005; Yao et al., 2015). At physiological ionic strength, the GTBM-mediated activation of Myo5a depends on the interaction between the GTD and RilpL2, which is regulated by Rab36 (Cao et al., 2019). Those findings are consistent with the three-dimensional structure of Myo5a-GTD and the folded structure of full-length Myo5a (Niu et al., 2022; Pylypenko et al., 2013; Wei et al., 2013), in both of which the GTBM-binding sites are buried at the GTD-GTD interface. Upon binding to the RH1 domain of RilpL2, the GTD exposes the GTBM-binding site (Wei et al., 2013). We therefore proposed that the binding of Rab36/RilpL2 to the GTD exposes the GTBM-binding site, thus facilitating GTBM to bind to the GTD and to activate the motor function of Myo5a (Cao et al., 2019).

The GTD/GTBM interaction is also required for the stable association between Myo5a and Mlph. The Myo5a tail construct containing all three Mlph-binding sites (the exon-F, the exon-G, and the GTD) produced dominant negative effect in melanocytes, and deleting the GTD abolished the dominant negative effect (Figure 7 and 8, and reference (X. Wu et al., 2002)).

The exon-F/EFBD and the exon-G/ABD interactions play a major role in the binding of Myo5a with Mlph. Although exon-F and exon-G are adjacent to each other, the exon-F/EFBD interaction and the exon-G/ABD interaction do not interfere with each other. Rather, those two interactions act synergically. We observed that Myo5a-MTD, containing both exon-F and exon-G but lacking the GTD, did not generate a dilute-like phenotype in melanocytes, but was co-localized well with Mlph and partially with melanosomes. Deletion of either exon-F or exon-G substantially weakened the interaction between Myo5a-MTD and Mlph and decreased the colocalization of Myo5a-MTD with Mlph, indicating the both exon-F and exon-G are required for the colocalization.

Our observation that Myo5a-MTD, containing both exon-F and exon-G, was co-localized partially with melanosomes seems to contradict the early work from Hammer laboratory, which showed that MC STK (a Myo5a fragment contains both exon-F and exon-G) did not exhibit any tendency to co-localize with melanosomes (X. Wu et al., 2002). However, careful examining their image (Figure 5, in reference(X. Wu et al., 2002)) reveals a partial colocalization of MC STK with melanosomes, particularly at the perinuclear region. It is likely that some melanosome-bound Mlph molecules are unoccupied, some interact with Myo5a via the exon-F/EFBD and the exon-G/ABD interactions but not the GTD/GTBM interaction, and some interact with Myo5a via three interactions. In the former two cases, Myo5a-MTD would be able to bind to the melanosome via Mlph. We therefore conclude that presence of both exon-F and exon-G is sufficient for Myo5a to associate with Mlph, but insufficient for substituting the melanosome-bound Myo5a molecules which bind to Mlph via three distinct interactions.

As discussed above, the GTBM-binding site is buried at the GTD-GTD interface in the folded state of Myo5a, thus is inaccessible for Mlph, and the opening of GTBM-site depends on the interaction with Rab36/RilpL2. On the other hand, the exon-F and the exon-G are likely exposed. We therefore propose that the folded Myo5a first attaches to Mlph via the exon-F/EFBD and exon-G/ABD interactions, then interacts with Rab36/RilpL2 to open the GTBM-site, and finally interacts with the GTBM, forming the extended conformation and being activated.

One interesting finding of this study is that Mlph-ABD was able to separately interact with the exon-G of Myo5a or actin filament, but unable to interact with both of them simultaneously. In other words, Mlph-ABD binds to either exon-G or actin filament. This is consistent with the geometry of Myo5a, in which exon-G is located far from the motor domain, which interacts with actin filament to produce motility. Given the small size of Mlph-ABD, it is unlikely that Mlph-ABD is able to bridge the exon-G at one end of Myo5a and actin filament which associates with the motor domain located at the other end of Myo5a. An unsolved issue is how Mlph-ABD's interactions with exon-G and actin filament are regulated. *In vitro* studies suggest that the interaction between Mlph-ABD and actin filament might be regulated by phosphorylation (Oberhofer et al., 2017).

Based on our current finding and previous studies on the interaction between Myo5a and its associated proteins, we propose following model for the Mlph-mediated Myo5a transportation of melanosome (Figure 9). At stage 1, Mlph associates with melanosome via its interaction with Rab27a, which directly binds to the membrane of melanosome; the unattached Myo5a is in a folded conformation, in which the GTD binds to and inhibits the motor domain. At stage 2, Mlph interacts with the folded Myo5a via the interactions of EFBD/exon-F and ABD/exon-G; the attached Myo5a is still in folded conformation, because the GTBM-binding surface in the GTD is buried at the GTD-GTD interface. At stage 3, the buried GTBM-binding surface between the GTD-GTD interface is exposed and thus facilitate the binding of GTBM, causing the dissociation of the GTD from the motor domain and inducing the extended conformation of Myo5a (This step is probably regulated by the binding of Rab36/RilpL2 to the GTD). At stage 4, Mlph-ABD dissociates from exon-G and then binds to actin filament, thus enhancing the processive movement of Myo5a (This step might be regulated by the phosphorylation of Mlph-ABD). The interaction between Mlph-ABD and actin filament is regulated by phosphorylation (Oberhofer et al., 2017).

Melanosomes in melanocytes are matured through a serial of well-defined morphological steps, from melanin-lacking premelanosomes to blackened melanosomes with melanin fully loaded (Raposo & Marks, 2007). During this maturation process, melanosomes undergo microtubule and actin-based transport towards the cell periphery, mediated by different Rab proteins and their effectors (Fukuda, 2021). For example, Rab27a mainly associates with intermediate and mature melanosomes (Jordens et al., 2006). The melanosome-bound Rab27a in GTP-bound state binds to Mlph, which in turn recruits Myo5a (X. S. Wu et al., 2002). We propose that the recruitment of Myo5a by Mlph consists of multiple stages. We expect that Myo5a-MTD, containing both exon-F and exon-G, is able to bind to Mlph at stage 1 and 2, but not at stage 3 and 4, and that Myo5a-Tail, containing all three Mlph-binding sites, is able to bind to Mlph at all four stages.

In conclusion, we demonstrate a direct interaction between the exon-G of Myo5a and the ABD of Mlph, which is essential for the tight binding of Myo5a to Mlph both *in vitro* and *in vivo*. We expect that the melanosomal recruitment and activation of Myo5a are a highly coordinated process mediated by three interactions between Myo5a and Mlph, i.e., the exon-F/EFBD interaction, the exon-G/ABD interaction, and the GTD/GTBM interactions.

337 **EXPERIMENTAL PROCEDURES**

338 **Materials**

339 Restriction enzymes and modifying enzymes were purchased from New England Biolabs (Beverly,
340 MA), unless indicated otherwise. Actin was prepared from rabbit skeletal muscle acetone powder according
341 to Spudich and Watt (Spudich & Watt, 1971). Ni-NTA agarose was purchased from Qiagen (Hilden,
342 Germany). Anti-Flag M2 affinity agarose and HPR conjugated anti-Flag M2 antibody were from Sigma Co.
343 (St. Louis, MO). EGFP and β-Tubulin antibody was purchased from PTMBio (Hangzhou, China).
344 Glutathione(GSH)-Sepharose 4 Fast Flow was from GE Healthcare. FLAG peptide (DYKDDDDK) was
345 synthesized by Augct Co. (Beijing, China). Oligonucleotides were synthesized by Invitrogen Co. (Beijing,
346 China).

347 **Proteins**

348 All Myo5a constructs in this study were created from a melanocyte type Myo5a (Li et al., 2005). The
349 recombinant proteins of truncated Myo5a containing an N-terminal His-tag and Flag-tag were expressed in
350 BL21(DE3) E. coli. The cDNA of truncated Myo5a were amplified by using high-fidelity FastPfu DNA
351 polymerase (TransGen) with Myo5a cDNA as template (Li et al., 2005), and subcloned into pET30HFa (a
352 modified pET30a vector encoding His-tag and Flag-tag). To improve the expression of short peptides of
353 truncated Myo5a, including Myo5a(1411-1467) and Myo5a(1436-1467), the cDNA of Trx-1 (Genbank ID:
354 P0AA25) was inserted between the Flag-tag sequence and the cDNA of truncated Myo5a in pET30HFa.
355 Myo5a-MTDΔF were created by using overlap extension PCR with Myo5a-MTD/pFast FTb as template
356 and inserted into pET30HFa. The recombinant proteins were expressed in BL21(DE3) *E. coli* as His-Flag
357 tagged proteins were purified by Ni-agarose affinity chromatography using standard procedures. We also
358 produced an N-terminal His-tagged and Flag-tagged Myo5a-MTD using baculovirus/Sf9 system. The
359 cDNA of Myo5a-MTD was subcloned into the baculovirus transfer vector pFastHFTb (a modified
360 pFastHTb vector containing the His-tag and Flag-tag sequence). Recombinant baculovirus was generated
361 using Bac-to-Bac system. The Myo5a-MTD expressed in Sf9 insect cells was purified by Anti-FLAG M2
362 affinity chromatography (Li et al., 2008).

363 Three truncated Mlph constructs containing an N-terminal GST-tag, including Mlph-ABD (residues
364 401-590), Mlph-ΔRBD (residues 148-590), Mlph-ΔRBDΔABD (residues 148-400), were created by
365 subcloning the cDNAs of truncated Mlph into pGEX4T1 vector using BamHI and XhoI sites. Mlph-EFBD
366 (residues 241-400) having an N-terminal His-tag and Flag-tag was created by the cDNA of Mlph-EFBD
367 subcloning into pET30HFa vector using EcoRI and HindIII sites. Point mutations were created using Fast
368 Mutagenesis System (TransGen) according to the manufacturer's instructions. The recombinant proteins
369 were expressed in BL21(DE3) *E. coli* as His-Flag tagged proteins (in pET30HFa vector) or GST tagged
370 proteins (in pGEX4T1 vector), and purified by Ni-agarose affinity chromatography or GSH-Sepharose
371 affinity chromatography using standard procedures.

372 **Protein pulldown assay**

373 GST pulldown assays were performed as described previously (Zhang et al., 2016). For GST pulldown
374 of Myo5a-MTD with GST-Mlph-ABD, GSH-Sepharose beads (10 μl) were mixed with 95 μl of 2 μM
375 GST-Mlph-ABD, 4 μM Myo5a-MTD truncations in Pulldown Buffer-I (5 mM Tris-HCl (pH 7.5), 100 mM
376 NaCl, 1 mM DTT, and 1 mM EGTA, 0.1% NP-40) with rotation at 4 °C for 2 h. The GSH-Sepharose beads
377 were then washed three times with 200 μl of Wash Buffer-I (10 mM Tris-HCl (pH 7.5), 100 mM NaCl, 1
378 mM DTT, and 1 mM EGTA, 0.1% NP-40), before eluted by Elution Buffer (10 mM GSH, 50 mM Tris-HCl
379 (pH 8.0), 1 mM DTT, and 200 mM NaCl). For GST pulldown of Myo5a-MTD with GST-Mlph-ΔRBD,
380 GSH-Sepharose beads (10 μl) were mixed with 95 μl of 2 μM GST-Mlph-ΔRBD, 4 μM Myo5a-MTD in
381 Pulldown Buffer-II (5 mM Tris-HCl (pH 7.5), 100 mM NaCl, 1 mM DTT, and 1 mM EGTA) with rotation
382 at 4 °C for 2 h. The GSH-Sepharose beads were washed three times with 200 μl of Wash Buffer-II (10 mM
383 Tris-HCl (pH 7.5), 100 mM NaCl, 1 mM DTT, and 1 mM EGTA) and then eluted by Elution Buffer.

384 For Flag pulldown assay, Flag-Myo5a-MTD (0.5 μM) was incubated with 1 μM GST-tagged Mlph
385 truncations in Pulldown Buffer I and rotated at 4 °C for 2 h, mixed with 10 μl of anti-FLAG M2 agarose.
386 The anti-FLAG M2 agarose were washed three times with 200 μl of Wash Buffer I. The bound proteins
387 were eluted twice with 20 μl of 0.1 mg/ml FLAG peptide in Wash Buffer I.

388 The inputs and the eluted proteins were analyzed by SDS-PAGE and visualized by Coomassie Brilliant
389 Blue (CBB) staining or Western blotting using the indicated antibody. The amounts of pulldowned proteins
390 were quantified using ImageJ (version 1.42Q), and their molar ratios were calculated on the basis of their
391 molecular masses.

392 **Microscale Thermophoresis**

393 The microscale thermophoresis (MST) assay of the interaction between Mlph-ABD with Myo5a-MTD or
394 Myo5a-MTDΔG were carried out in a Monolith NT.115 instrument (NanoTemper Technologies, Germany)
395 at 25°C. Mlph-ABD was labelled with ATTO 488 NHS Ester dye (ATTO-TEC) according to the
396 manufacturer's instructions. The Mlph-ABD was kept at a constant concentration of 20 nM. Two-fold
397 dilution series (16 in total) of the Myo5a-MTD (50 μM) or Myo5a-MTDΔG (50 μM) were performed in the
398 MST buffer (50 mM Tris-HCl pH 7.8, 100 mM NaCl, 10 mM $MgCl_2$, 0.05% Tween 20). The dissociation
399 constant K_d was obtained using Monolith Affinity Analysis v2.2.4 software.

400 **Actin cosedimentation assay**

401 Rabbit skeletal actin (2 μM) and Mlph-ABD (4 μM) was incubated in a 60 μL solution of 20 mM Tris-HCl
402 (pH 7.5), 100 mM NaCl, 1 mM EGTA, and 1 mM DTT at 4 °C for 20 min with or without Myo5a-MTD (2
403 μM). In addition, Myo5a-MTD (0-8 μM) was incubated with rabbit skeletal actin (2 μM) and Mlph-ABD (1
404 μM) in a 60 μL solution of 20 mM Tris-HCl (pH 7.5), 100 mM NaCl, 1 mM EGTA, and 1 mM DTT at 4 °C
405 for 20 min. The mixtures were centrifuged at 85,000 rpm (Beckman Optima MAX-XP, TLA-120.1 rotor)
406 for 15 min at 4 °C. Equal portions of the pellet and the supernatant were subjected to SDS−PAGE and
407 Coomassie brilliant blue staining.

408 **Melanophilin antibody**

409 To generate a polyclonal antibody against melanophilin, the sequence encoding residues 147-428 of
410 melanophilin (Mlph-147-428) was amplified by PCR using a full-length mouse melanophilin cDNA as
411 template. The PCR product was cloned into pET30a vector and pGEX4T2 vector and expressed in E. coli as
412 His-tagged protein (His-Mlph-147-428) and GST-tagged protein (GST-Mlph-147-428), respectively.
413 His-Mlph-147-428 was purified using Ni-NTA agrose chromatography and used for immunizing rabbit.
414 GST-Mlph-147-428 was purified using GSH-Sepharose chromatography. Mlph antibody was
415 affinity-purified from immune sera over a column of GST-Mlph-147-428 coupled to cyanogen
416 bromide-activated Sepharose 4B (GE Healthcare) by standard procedure.

417 **Plasmid constructions for melanocyte transfection**

418 Myo5a-Tail/pEGFP-C1 was produced as described previously(X. Wu et al., 2002).
419 Myo5a-TailΔF/pEGFP-C1 and Myo5a-TailΔG/pEGFP-C1 were created by overlapping PCR using
420 Myo5a-Tail/pEGFP-C1 as template. Myo5a-MTD/pEGFP-C1 and Myo5a-MTDΔG/pEGFP-C1 were
421 produced by PCR amplification using Myo5a-Tail/pEGFP-C1 as template. Myo5a-MTDΔF/pEGFP-C1 was
422 created by subcloning from Myo5a-MTDΔF/pET30a into pEGFP-C1.

423 **Melanocyte culture and transfection**

424 The immortal mouse melanocyte cell line melan-a, kindly provided by Dr. Dorothy Bennett, was
425 cultured as described (Bennett et al., 1987). Briefly, melan-a cells were cultured in RPMI 1640 medium
426 (HyClone) supplemented with 10% fetal bovine serum, 200 nM phorbol 12-myristate 13-acetate and
427 penicillin/streptomycin (1% v/v) in humidified chamber (37 °C, 5% CO2 incubator). Melan-a cells were

428 passaged at 3–4 day intervals. Hieff Trans® Universal Transfection Reagent (Yeasen) was used for
429 transfection of pEGFP-C1 plasmids into melan-a cells according to the manufacturer's instructions.

430 **Immunocytochemistry**

431 For immunofluorescence staining, melan-a cells were plated on the coverslips. After 24 h culturing, cells
432 were transfected of pEGFP-C1 plasmids. Two days after transfection, the cells were fixed using 4%
433 paraformaldehyde for 20 min, then permeabilized with 0.4% Triton-X in PBS for 15 min. Subsequently, the
434 coverslips were blocked with 1% BSA for 1 h. Melan-a cells were incubated with rabbit antibody against
435 Mlph overnight. Coverslips were washed with PBS for 3 times and then incubated for 1 h at room
436 temperature with secondary antibodies (anti-rabbit IgG coupled with DyLight 549, Jackson). Nuclei were
437 counter-stained with DAPI. coverslips were fixed on glass slides with Fluoromount-GTM (Yeasen). The
438 images were captured by Leica STELLARIS 5 fluorescence microscope.
439
440

441 **FOOTNOTES**

442 The abbreviations used are: ABD, actin-binding domain of melanophilin; CaM, calmodulin; EFBD,
443 exon-F-binding domain of melanophilin; GSH, glutathione; GST, glutathione S-transferase; GTBM,
444 GTD-binding motif of melanophilin; GTD, globular tail domain of myosin-5a; Mlph, melanophilin; MTD,
445 middle tail domain of myosin-5a; Myo5a, myosin-5a.

446

447 **ACKNOWLEDGEMENTS**

448 We thank Dr. Zheng Zhou (Institute of Biophysics, Chinese Academy of Sciences) for advice on
449 myosin-5a/melanophilin interaction. This work was supported by the National Natural Science Foundation
450 of China (31970657).

451

452 **CONFLICT OF INTEREST**

453 The authors declare that they have no conflicts of interest with the contents of this article.
454

455 **AUTHOR CONTRIBUTIONS**

456 XdL conceived the study. JP performed most experiments with help from RZ. LLY, NZ and JZ performed
457 the initial experiments demonstrating the interaction between Mlph-ABD and Myo5a tail. QJC prepared
458 melanophilin antibody. SP participated in preparation of recombinant proteins and pulldown assays. JP and
459 XdL designed the study, analyzed the data and wrote the manuscript.
460
461

REFERENCES

Bennett, D. C., Cooper, P. J., & Hart, I. R. (1987). A line of non-tumorigenic mouse melanocytes, syngeneic with the B16 melanoma and requiring a tumour promoter for growth. *Int J Cancer*, *39*(3), 414-418. http://www.ncbi.nlm.nih.gov/entrez/query.fcgi?cmd=Retrieve&db=PubMed&dopt=Citation&list_uids=3102392

Cao, Q. J., Zhang, N., Zhou, R., Yao, L. L., & Li, X. D. (2019). The cargo adaptor proteins RILPL2 and melanophilin co-regulate myosin-5a motor activity. *J Biol Chem*, *294*(29), 11333-11341. https://doi.org/10.1074/jbc.RA119.007384

Fukuda, M. (2021). Rab GTPases: Key players in melanosome biogenesis, transport, and transfer. *Pigment Cell Melanoma Res*, *34*(2), 222-235. https://doi.org/10.1111/pcmr.12931

Fukuda, M., & Itoh, T. (2004). Slac2-a/melanophilin contains multiple PEST-like sequences that are highly sensitive to proteolysis. *J Biol Chem*, *279*(21), 22314-22321. https://doi.org/10.1074/jbc.401791200

Fukuda, M., & Kuroda, T. S. (2002). Slac2-c (synaptotagmin-like protein homologue lacking C2 domains-c), a novel linker protein that interacts with Rab27, myosin Va/VIIa, and actin. *J Biol Chem*, *277*(45), 43096-43103. https://doi.org/10.1074/jbc.M203862200

Fukuda, M., Kuroda, T. S., & Mikoshiba, K. (2002). Slac2-a/melanophilin, the missing link between Rab27 and myosin Va: implications of a tripartite protein complex for melanosome transport. *J Biol Chem*, *277*(14), 12432-12436. https://doi.org/10.1074/jbc.C200005200

Geething, N. C., & Spudich, J. A. (2007). Identification of a minimal myosin Va binding site within an intrinsically unstructured domain of melanophilin. *J Biol Chem*, *282*(29), 21518-21528. https://doi.org/10.1074/jbc.M701932200

Huang, J. D., Mermall, V., Strobel, M. C., Russell, L. B., Mooseker, M. S., Copeland, N. G., & Jenkins, N. A. (1998). Molecular genetic dissection of mouse unconventional myosin-VA: tail region mutations. *Genetics*, *148*(4), 1963-1972. https://doi.org/10.1093/genetics/148.4.1963

Hume, A. N., A.K. Tarafder, J.S. Ramalho, E.V. Sviderskaya, and M.C. Seabra. (2006). A Coiled-Coil Domain of Melanophilin Is Essential forMyosin Va Recruitment and Melanosome Transport inMelanocytes. *Molecular Biology of the Cell*, *17*, 4720-4735. https://doi.org/10.1091/mbc.E06-05-0457)

Hume, A. N., Collinson, L. M., Rapak, A., Gomes, A. Q., Hopkins, C. R., & Seabra, M. C. (2001). Rab27a regulates the peripheral distribution of melanosomes in melanocytes. *J Cell Biol*, *152*(4), 795-808. http://www.ncbi.nlm.nih.gov/entrez/query.fcgi?cmd=Retrieve&db=PubMed&dopt=Citation&list_uids=11266470

Hume, A. N., & Seabra, M. C. (2011). Melanosomes on the move: a model to understand organelle dynamics. *Biochem Soc Trans*, *39*(5), 1191-1196. https://doi.org/10.1042/BST0391191

Ikebe, M. (2008). Regulation of the function of mammalian myosin and its conformational change. *Biochem Biophys Res Commun*, *369*(1), 157-164. https://doi.org/10.1016/j.bbrc.2008.01.057

Ishida, M., Arai, S. P., Ohbayashi, N., & Fukuda, M. (2014). The GTPase-deficient Rab27A(Q78L) mutant inhibits melanosome transport in melanocytes through trapping of Rab27A effector protein Slac2-a/melanophilin in their cytosol: development of a novel melanosome-targetinG tag. *J Biol Chem*, *289*(16), 11059-11067. https://doi.org/10.1074/jbc.M114.552281

Jordens, I., Westbroek, W., Marsman, M., Rocha, N., Mommaas, M., Huizing, M., Lambert, J., Naeyaert, J. M., & Neefjes, J. (2006). Rab7 and Rab27a control two motor protein activities involved in melanosomal transport. *Pigment Cell Res*, *19*(5), 412-423. https://doi.org/10.1111/j.1600-0749.2006.00329.x

Krementsov, D. N., Krementsova, E. B., & Trybus, K. M. (2004). Myosin V: regulation by calcium, calmodulin, and the tail domain. *J Cell Biol*, *164*(6), 877-886. http://www.ncbi.nlm.nih.gov/entrez/query.fcgi?cmd=Retrieve&db=PubMed&dopt=Citation&list_uids=15007063

Kuroda, T. S., Ariga, H., & Fukuda, M. (2003). The actin-binding domain of Slac2-a/melanophilin is required for melanosome distribution in melanocytes. *Mol Cell Biol*, *23*(15), 5245-5255. http://www.ncbi.nlm.nih.gov/entrez/query.fcgi?cmd=Retrieve&db=PubMed&dopt=Citation&list_uids=12861011

Kuroda, T. S., Ariga, H., & Fukuda, M. (2003). The Actin-Binding Domain of Slac2-a/Melanophilin Is Required for Melanosome Distribution in Melanocytes. *Molecular and Cellular Biology*, *23*(15), 5245-5255. https://doi.org/10.1128/mcb.23.15.5245-5255.2003

Li, X. D., Ikebe, R., & Ikebe, M. (2005). Activation of myosin Va function by melanophilin, a specific docking partner of myosin Va. *J Biol Chem*, *280*(18), 17815-17822. https://doi.org/10.1074/jbc.M413295200

Li, X. D., Jung, H. S., Mabuchi, K., Craig, R., & Ikebe, M. (2006). The globular tail domain of myosin Va functions as an inhibitor of the myosin Va motor. *J Biol Chem*, *281*(31), 21789-21798. https://doi.org/10.1074/jbc.M602957200

Li, X. D., Jung, H. S., Wang, Q., Ikebe, R., Craig, R., & Ikebe, M. (2008). The globular tail domain puts on the brake to stop the ATPase cycle of myosin Va. *Proc Natl Acad Sci U S A*, *105*(4), 1140-1145. https://doi.org/10.1073/pnas.0709741105

Li, X. D., Mabuchi, K., Ikebe, R., & Ikebe, M. (2004). Ca2+-induced activation of ATPase activity of myosin Va is accompanied with a large conformational change. *Biochem Biophys Res Commun*, *315*(3), 538-545. http://www.ncbi.nlm.nih.gov/entrez/query.fcgi?cmd=Retrieve&db=PubMed&dopt=Citation&list_uids=14975734

Lindsay, A. J., & McCaffrey, M. W. (2014). Myosin Va is required for the transport of fragile X mental retardation protein (FMRP) granules. *Biol Cell*, *106*(2), 57-71. https://doi.org/10.1111/boc.201200076

Liu, J., Taylor, D. W., Krementsova, E. B., Trybus, K. M., & Taylor, K. A. (2006). Three-dimensional structure of the myosin V inhibited state by cryoelectron tomography. *Nature*, *442*(7099), 208-211. https://doi.org/10.1038/nature04719

Mehta, A. D., Rock, R. S., Rief, M., Spudich, J. A., Mooseker, M. S., & Cheney, R. E. (1999). Myosin-V is a processive actin-based motor. *Nature*, *400*(6744), 590-593. https://doi.org/10.1038/23072

Nagashima, K., Torii, S., Yi, Z., Igarashi, M., Okamoto, K., Takeuchi, T., & Izumi, T. (2002). Melanophilin directly links Rab27a and myosin Va through its distinct coiled-coil regions. *FEBS Lett*, *517*(1-3), 233-238. http://www.ncbi.nlm.nih.gov/entrez/query.fcgi?cmd=Retrieve&db=PubMed&dopt=Citation&list_uids=12062444

Niu, F., Liu, Y., Sun, K., Xu, S., Dong, J., Yu, C., Yan, K., & Wei, Z. (2022). Autoinhibition and activation mechanisms revealed by the triangular-shaped structure of myosin Va. *Sci Adv*, *8*(49), eadd4187. https://doi.org/10.1126/sciadv.add4187

Oberhofer, A., Spieler, P., Rosenfeld, Y., Stepp, W. L., Cleetus, A., Hume, A. N., Mueller-Planitz, F., & Okten, Z. (2017). Myosin Va's adaptor protein melanophilin enforces track selection on the microtubule and actin networks in vitro. *Proc Natl Acad Sci U S A*, *114*(24), E4714-E4723. https://doi.org/10.1073/pnas.1619473114

Provance, D. W., Jr., Wei, M., Ipe, V., & Mercer, J. A. (1996). Cultured melanocytes from dilute mutant mice exhibit dendritic morphology and altered melanosome distribution. *Proceedings of the National Academy of Sciences of the United States of America*, *93*(25), 14554-14558.

Pylypenko, O., Attanda, W., Gauquelin, C., Lahmani, M., Coulibaly, D., Baron, B., Hoos, S., Titus, M. A., England, P., & Houdusse, A. M. (2013). Structural basis of myosin V Rab GTPase-dependent cargo recognition. *Proc Natl Acad Sci U S A*, *110*(51), 20443-20448. https://doi.org/10.1073/pnas.1314329110

Raposo, G., & Marks, M. S. (2007). Melanosomes--dark organelles enlighten endosomal membrane transport. *Nat Rev Mol Cell Biol*, *8*(10), 786-797. https://doi.org/nrm2258 [pii]
10.1038/nrm2258

Rudolf, R., Bittins, C. M., & Gerdes, H. H. (2011). The role of myosin V in exocytosis and synaptic plasticity. *J Neurochem*, *116*(2), 177-191. https://doi.org/10.1111/j.1471-4159.2010.07110.x

Sckolnick, M., Krementsova, E. B., Warshaw, D. M., & Trybus, K. M. (2013). More than just a cargo adapter, melanophilin prolongs and slows processive runs of myosin Va. *J Biol Chem*, *288*(41), 29313-29322. https://doi.org/10.1074/jbc.M113.476929

Seperack, P. K., Mercer, J. A., Strobel, M. C., Copeland, N. G., & Jenkins, N. A. (1995). Retroviral sequences located within an intron of the dilute gene alter dilute expression in a tissue-specific manner. *EMBO Journal*, *14*(10), 2326-2332.

Spudich, J. A., & Watt, S. (1971). The regulation of rabbit skeletal muscle contraction. I. Biochemical studies of the interaction of the tropomyosin-troponin complex with actin and the proteolytic fragments of myosin. *J Biol Chem*, *246*(15), 4866-4871. http://www.ncbi.nlm.nih.gov/entrez/query.fcgi?cmd=Retrieve&db=PubMed&dopt=Citation&list_uids=4254541

Strom, M., Hume, A. N., Tarafder, A. K., Barkagianni, E., & Seabra, M. C. (2002). A family of Rab27-binding proteins. Melanophilin links Rab27a and myosin Va function in melanosome transport. *J Biol Chem*, *277*(28), 25423-25430. https://doi.org/10.1074/jbc.M202574200

Thirumurugan, K., Sakamoto, T., Hammer, J. A., Sellers, J. R., & Knight, P. J. (2006). The cargo-binding domain regulates structure and activity of myosin 5. *Nature*, *442*(7099), 212-215. https://doi.org/10.1038/nature04865

573 Wandinger-Ness, A., & Zerial, M. (2014). Rab proteins and the compartmentalization of the endosomal system. *Cold*
574 *Spring Harb Perspect Biol*, *6*(11), a022616. https://doi.org/10.1101/cshperspect.a022616
575 Wang, F., Thirumurugan, K., Stafford, W. F., Hammer, J. A., 3rd, Knight, P. J., & Sellers, J. R. (2004). Regulated
576 conformation of myosin V. *J Biol Chem*, *279*(4), 2333-2336. https://doi.org/10.1074/jbc.C300488200
577 Wei, Q., Wu, X., & Hammer, J. A., 3rd. (1997). The predominant defect in dilute melanocytes is in melanosome
578 distribution and not cell shape, supporting a role for myosin V in melanosome transport. *J Muscle Res Cell*
579 *Motil*, *18*(5), 517-527.
580 http://www.ncbi.nlm.nih.gov/entrez/query.fcgi?cmd=Retrieve&db=PubMed&dopt=Citation&list_uids=9350
581 005
582 Wei, Z., Liu, X., Yu, C., & Zhang, M. (2013). Structural basis of cargo recognitions for class V myosins. *Proc Natl*
583 *Acad Sci U S A*, *110*(28), 11314-11319. https://doi.org/10.1073/pnas.1306768110
584 Wu, X., Bowers, B., Rao, K., Wei, Q., & Hammer, J. A. r. (1998). Visualization of melanosome dynamics within
585 wild-type and dilute melanocytes suggests a paradigm for myosin V function In vivo. *J Cell Biol*, *143*(7),
586 1899-1918.
587 Wu, X., & Hammer, J. A. (2014). Melanosome transfer: it is best to give and receive. *Curr Opin Cell Biol*, *29*, 1-7.
588 https://doi.org/10.1016/j.ceb.2014.02.003
589 Wu, X., Rao, K., Bowers, M. B., Copeland, N. G., Jenkins, N. A., & Hammer, J. A., 3rd. (2001). Rab27a enables
590 myosin Va-dependent melanosome capture by recruiting the myosin to the organelle. *Journal of Cell Science*,
591 *114*(Pt 6), 1091-1100.
592 Wu, X., Wang, F., Rao, K., Sellers, J. R., & Hammer, J. A., 3rd. (2002). Rab27a is an essential component of
593 melanosome receptor for myosin Va. *Mol Biol Cell*, *13*(5), 1735-1749.
594 https://doi.org/10.1091/mbc.01-12-0595
595 Wu, X. S., Rao, K., Zhang, H., Wang, F., Sellers, J. R., Matesic, L. E., Copeland, N. G., Jenkins, N. A., & Hammer, J.
596 A., 3rd. (2002). Identification of an organelle receptor for myosin-Va. *Nat Cell Biol*, *4*(4), 271-278.
597 https://doi.org/10.1038/ncb760
598 Wu, X. S., Tsan, G. L., & Hammer, J. A., 3rd. (2005). Melanophilin and myosin Va track the microtubule plus end on
599 EB1. *J Cell Biol*, *171*(2), 201-207. https://doi.org/10.1083/jcb.200503028
600 Yao, L. L., Cao, Q. J., Zhang, H. M., Zhang, J., Cao, Y., & Li, X. D. (2015). Melanophilin Stimulates Myosin-5a
601 Motor Function by Allosterically Inhibiting the Interaction between the Head and Tail of Myosin-5a. *Sci Rep*,
602 *5*, 10874. https://doi.org/10.1038/srep10874
603 Yoshimura, A., Fujii, R., Watanabe, Y., Okabe, S., Fukui, K., & Takumi, T. (2006). Myosin-Va facilitates the
604 accumulation of mRNA/protein complex in dendritic spines. *Curr Biol*, *16*(23), 2345-2351.
605 https://doi.org/10.1016/j.cub.2006.10.024
606 Zhang, N., Yao, L. L., & Li, X. D. (2018). Regulation of class V myosin. *Cell Mol Life Sci*, *75*(2), 261-273.
607 https://doi.org/10.1007/s00018-017-2599-5
608 Zhang, W. B., Yao, L. L., & Li, X. D. (2016). The Globular Tail Domain of Myosin-5a Functions as a Dimer in
609 Regulating the Motor Activity. *J Biol Chem*, *291*(26), 13571-13579.
610 https://doi.org/10.1074/jbc.M116.724328

611

612 **FIGURE LEGENDS**

613 **Figure 1. The actin-binding domain of melanophilin (Mlph-ABD) interacts with the middle tail**
614 **domain (MTD) of Myo5a.** (A) Diagram of the melanocyte-spliced isoform of Myo5a. Myo5a-MTD,
615 Myo5a coiled-coils (residues 1106-1469). IQ, the CaM binding site; GTD, the C-terminal globular tail
616 domain. In blue box is the sequence of exon-F and -G, annotated with the predicted coiled-coil heptad
617 repeats. (B) Diagram of melanophilin (Mlph). RBD, Rab27a-binding domain; GTBM, globular tail
618 domain-binding motif; EFBD, exon-F binding domain; ABD, actin-binding domain. (C, D) GST pulldown
619 of GST-Mlph-ABD with the N-terminus truncated (C) or the C-terminus truncated (D) with
620 Flag-Myo5a-MTD. GST-Mlph-ABD constructs were bound to GSH-Sepharose and then incubated with
621 Flag-Myo5a-MTD. The GSH-Sepharose-bound proteins were eluted by GSH and analyzed by Western blot
622 using anti-Flag antibody. The inputs were analyzed with SDS-PAGE and visualized by Coomassie brilliant

623 blue (CBB) staining. GST was used as negative control. Note: The Sf9 cell-expressed Myo5a-MTD was
624 used in the GST pulldown assays shown in this figure.
625 **Figure 1-Source data 1** Original and uncropped gels and blots for Figure 1C.
626 **Figure 1-Source data 2** Original and uncropped gels and blots for Figure 1D.
627

628 **Figure 2. The exon-G of Myo5a interacts with Mlph-ABD.** (A) Summary of the interactions between
629 the truncated Myo5a constructs and Mlph-ABD based on the GST pulldown assay shown in Figure S1. +,
630 strong interaction; +/-, weak interaction; -, no interaction. (B) Deletion of the C-terminal portion of exon-G
631 abolishes the interaction between Myo5a-MTD and Mlph-ABD. (C) Deletion of the C-terminal portion of
632 exon-G does not affect the interaction between Myo5a-MTD and Mlph-EFBD. GST pulldown assays were
633 performed using GST-Mlph-ABD and Flag-Myo5a-MTD variants. The GSH-Sepharose-bound proteins
634 were eluted by GSH and analyzed by Western blot using anti-FLAG antibody; the inputs were analyzed
635 with SDS-PAGE and visualized by Coomassie brilliant blue (CBB) staining.
636 **Figure 2-Source data 1** Original and uncropped gels and blots for Figure 2B.
637 **Figure 2-Source data 2** Original and uncropped gels and blots for Figure 2C.

638

639 **Figure 3. Identification of the key residues for the exon-G/ABD interaction.** (A) Dissociation constant
640 (K_d) of Myo5a-MTD or Myo5a-MTDΔG binding to Mlph-ABD measured by MST. The solid curve was fit
641 to the standard K_d-fit function. Bars represent Standard Error. (B) Ionic strength dependence of the
642 interaction between Myo5a-MTD and Mlph-ABD. GST pulldown was performed using GST-Mlph-ABD
643 and Flag-Myo5a-MTD in the presence of different concentrations of NaCl. (C) Sequence alignments of the
644 regions in Mlph-ABD essential for binding to Myo5a-MTD. Conserved charged residues are indicated. (D)
645 Sequence alignments of the C-terminal portion of exon-G, an essential region for binding to Mlph-ABD.
646 Two conserved basic residues (K1456 and K1460) are indicated. (E) Effects of alanine mutation of the
647 conserved charged residues in Mlph-ABD on the interaction with Myo5a-MTD. E449A and E452A
648 mutations in Mlph abolished the interaction between Mlph-ABD and Myo5a-MTD. (F) Effects of K1456A
649 and K1460A mutations of Myo5a-MTD on the interaction with Mlph-ABD.
650 **Figure 3-Source data 1** Original MST data for Figure 3A.
651 **Figure 3-Source data 2** Original and uncropped gels and blots for Figure 3B.
652 **Figure 3-Source data 3** Original and uncropped gels and blots for Figure 3E.
653 **Figure 3-Source data 4** Original and uncropped gels and blots for Figure 3F.
654

655 **Figure 4. The exon-F/EFBD and the exon-G/ABD interactions act synergistically.** (A) Myo5a-MTD
656 bridges between Mlph-ABD and Mlph-EFBD. Upper, diagram shows Myo5a-MTD binds to both the EFBD
657 and the ABD of Mlph. Lower, GST pulldown assays of GST-Mlph-ABD and Flag-Mlph-EFBD with or
658 without Flag-Myo5a-MTD. (B) Both exon-F and exon-G of Myo5a-MTD are required for the strong
659 interaction with Mlph-ΔRBD. GST pulldown of GST-Mlph-ΔRBD with Flag-Myo5a-MTD variants. (C)
660 ABD is essential for the strong interaction between Mlph-ΔRBD and Myo5a-MTD. The input samples were
661 analyzed by SDS-PAGE and visualized by CBB staining. The pulled down samples were analyzed by
662 Western blot using anti-Flag antibody (A and B) or by SDS-PAGE with CBB staining (C).
663 **Figure 4-Source data 1** Original and uncropped gels and blots for Figure 4A.
664 **Figure 4-Source data 2** Original and uncropped gels and blots for Figure 4B.
665 **Figure 4-Source data 3** Original and uncropped gels for Figure 4C.

666

667 **Figure 5. Myo5a-MTD antagonizes the interaction between Mlph-ABD and actin.** (A)
668 GST-Mlph-ABD and/or Flag-Myo5a-MTD were incubated with actin and then subjected to
669 ultracentrifugation. The supernatants (S) and the pellets (P) were analyzed by SDS-PAGE (10%) with CBB

670 staining. (B) GST-Mlph-ABD was incubated with actin in the presence of different concentrations of
671 Flag-Myo5a-MTD and then subjected to to ultracentrifugation. Upper panel, the supernatants (S) and the
672 pellets (P) were analyzed by SDS-PAGE (10%) with CBB staining. Lower panel, the amounts of
673 GST-Mlph-ABD co-sedimentated with actin in the presence of different concentration of
674 Flag-Myo5a-MTD were quantified based on the density in the SDS-PAGE. Data are the mean ± SD of three
675 independent experiments with one-way ANOVA with post-hoc Bonferroni test. **p<0.01, ****p<0.0001.
676 Note: a Sf9 cell-expressed Myo5a-MTD was used in the actin cosedimentation assays shown in this figure.
677 **Figure 5-Source data 1** Original and uncropped gels for Figure 5A.
678 **Figure 5-Source data 2** Original and uncropped gels and statistical data for Figure 5 B.

679

680 **Figure 6. Both E449 and E452 of Mlph are essential for the perinuclear distribution of melanosomes**
681 **induced by Mlph-ΔRBD overexpression.** Melan-a melanocytes were transfected to express
682 EGFP-Mlph-ΔRBD (WT, E449A, or E452A) or EGFP. The distribution of melanosomes in the transfected
683 melanocytes was imaged and the number of melanocytes with perinuclear distribution of melanosomes was
684 counted. (A) Typical images of melanocytes expressing EGFP alone, EGFP-Mlph-ΔRBD WT, E449A, or
685 E452A. Zooms are x 3. Cells are outlined with red dashed lines. Scale bars = 10 μm. The transfection
686 efficiences were 11% for EGFP (n=275), 9.2% for EGFP-Mlph-ΔRBD WT (n=194), 11.2% for E449A
687 (n=208), and 11.8% for E452A (n=267). n represents cell number. (B) The percentage of melanocytes
688 exhibiting perinuclear melanosome aggregation among the transfected melanocytes. Results are presented
689 as the mean ± SD of three independent experiments with one-way ANOVA with post-hoc Bonferroni test.
690 Each point represents the percentage of perinuclear distribution of EGFP fusion proteins expressing cells in
691 each fields. ****p<0.0001. (C) Western blot of the lysates of melan-a transfected with EGFP-Mlph-ΔRBD
692 WT, E449A, or E452A. The expressed EGFP fusion proteins were probed with the antibody against EGFP.
693 The relative band densities of EGFP-Mlph-ΔRBD WT, E449A, and E452A were 1, 1.29, and 1.25,
694 respectively. Correction of the transfection efficiencies of those three constructs (Figure 6A, Figure 6-figure
695 supplement) gave rise to the relative protein expression levels of each transfected cells as 1, 1.05, and 0.97
696 for EGFP-Mlph-ΔRBD WT, E449A, and E452A, respectively.
697 **Figure 6-Source data 1** Original and statistical data for Figure 6 B.
698 **Figure 6-Source data 2** Original and uncropped blots for Figure 6 C.
699

700 **Figure 7. Exon-G region of Myo5a is essential for the perinuclear distribution of melanosomes**
701 **induced by Myo5a-Tail overexpression.** (A) Diagram of Myo5a-Tail constructs used for transfecting
702 melan-a melanocytes. (B) Melan-a melanocytes were transfected to express EGFP-Myo5a-Tail and the
703 mutant. The distribution of melanosomes in the transfected melanocytes was imaged and the number of
704 melanocytes with perinuclear distribution of melanosomes was counted. (B) Typical images of melanocytes
705 expressing EGFP-Myo5a-Tail, its mutants, or EGFP. Cells are outlined with a dashed line. Scale bars = 10
706 μm. Zooms are x 3. (C) The percentages of melanocytes exhibiting perinuclear melanosome aggregation.
707 Data are the mean ± SD of three independent experiments with one-way ANOVA with post-hoc Bonferroni
708 test. ****p<0.0001. (D) Western blots of whole cell extracts prepared from melan-a melanocytes
709 transfected with each of the three Myo5a constructs EGFP fusion protein constructs probed with an
710 antibody against EGFP. Each point represents the percentages of perinuclear distribution of EGFP fusion
711 proteins expressing cells in each fields. (D) Western blot of the lysates of melan-a transfected with
712 EGFP-Myo5a-Tail or EGFP-Myo5a-TailΔG. The expressed EGFP fusion proteins were probed with the
713 antibody against EGFP. The relative band densities of EGFP-Myo5a-Tail and EGFP-Myo5a-TailΔG were 1
714 and 0.9, respectively. Correction of the transfection efficiencies of those three constructs (Figure 7B, Figure
715 7-figure supplement) gave rise to the relative protein expression levels of each transfected cells as 1, 0.93
716 for EGFP-Myo5a-Tail or EGFP-Myo5a-TailΔG, respectively.
717 **Figure 7-Source data 1** Original and statistical data for Figure 7 C.

718 **Figure 7-Source data 2** Original and uncropped blots for Figure 7 D.
719

720 **Figure 8. Effects of deletion of exon-F or exon-G on the localization of Myo5a-MTD in melan-a cells.**
721 Melan-a melanocytes were transfected to express EGFP-Myo5a-MTD (A), EGFP-Myo5a-MTDΔF (B), or
722 EGFP-Myo5a-MTDΔG (C) and stained for endogenous Mlph. Insets represent higher magnification
723 photomicrographs of a cell within the region outlined by frames. Scale bars = 10 μm.

724

725 **Figure 9. A model for the Mlph-mediated Myo5a transportation of melanosome.** The Mlph-mediated
726 Myo5a transportation of melanosome is comprised of four stages. At stage 1, Mlph associates with
727 melanosome via its interaction with Rab27a, which directly binds to the membrane of melanosome; the
728 unattached Myo5a is in a folded conformation, in which the GTD binds to and inhibits the motor domain.
729 At stage 2, Mlph interacts with the folded Myo5a via the interactions of EFBD/exon-F and ABD/exon-G;
730 the attached Myo5a is still in folded conformation, because the GTBM-binding surface in the GTD is buried
731 at the GTD-GTD interface. At stage 3, the buried GTBM-binding surface between the GTD-GTD interface
732 is exposed and thus facilitate the binding of GTBM, causing the dissociation of the GTD from the motor
733 domain and inducing the extended conformation of Myo5a (This step is probably regulated by the binding
734 of Rab36/RilpL2 to the GTD). At stage 4, Mlph-ABD dissociates from exon-G and then binds to actin
735 filament, thus enhancing the processive movement of Myo5a (This step might be regulated by the
736 phosphorylation of Mlph-ABD).

737
738 **Figure 2-figure supplement. Identification of the Mlph-ABD-binding site in the middle tail of**
739 **Myo5a.** GST pulldown assays were performed using GST-Mlph-ABD and FLAG-Myo5a-MTD variants.
740 The GSH-Sepharose-bound proteins were eluted by GSH and analyzed by Western blot using anti-FLAG
741 antibody; the inputs were analyzed with SDS-PAGE and visualized by Coomassie brilliant blue (CBB)
742 staining. (A) GST pulldown assays of GST-Mlph-ABD with Flag-Myo5a-MTD expressed in E. coli or Sf9
743 cells. (B and C) GST pulldown assay of GST-Mlph-ABD with Flag-tagged, truncated Myo5a tail.
744 **Figure 2-figure supplement Source data 1** Original and uncropped gels and blots for Figure 2-figure
745 supplement A.
746 **Figure 2-figure supplement Source data 2** Original and uncropped gels and blots for Figure 2-figure
747 supplement B.
748 **Figure 2-figure supplement Source data 3** Original and uncropped gels and blots for Figure 2-figure
749 supplement C.

750 **Figure 6-figure supplement.** Typical images of melanocytes expressing EGFP-Mlph-ΔRBD, its mutants,
751 or EGFP. Cells are outlined with a red dashed line. Scale bars = 10 μm. Zooms are x0.75.

752 **Figure 7-figure supplement.** Typical images of melanocytes expressing EGFP-Myo5a-Tail, its mutants, or
753 EGFP. Cells are outlined with a red dashed line. Scale bars = 10 μm. Zooms are x0.75.

754

755 **Figure 1-Source data 1** Original and uncropped gels and blots.

756 **Figure 1-Source data 2** Original and uncropped gels and blots.

757 **Figure 2-Source data 1** Original and uncropped gels and blots.

Figure 2-Source data 2 Original and uncropped gels and blots.

Figure 3-Source data 1 Original data.

Figure 3-Source data 2 Original and uncropped gels and blots.

Figure 3-Source data 3 Original and uncropped gels and blots.

Figure 3-Source data 4 Original and uncropped gels and blots.

Figure 4-Source data 1 Original and uncropped gels and blots.

Figure 4-Source data 2 Original and uncropped gels and blots.

Figure 4-Source data 3 Original and uncropped gels.

Figure 5-Source data 1 Original and uncropped gels.

Figure 5-Source data 2 Original and uncropped gels and data.

Figure 6-Source data 1 Original and statistical data.

Figure 6-Source data 2 Original and uncropped blots.

Figure 7-Source data 1 Original and statistical data.

Figure 7-Source data 2 Original and uncropped blots.

Figure 2-figure supplement Source data 1 Original and uncropped gels and blots.

Figure 2-figure supplement Source data 2 Original and uncropped gels and blots.

Figure 2-figure supplement Source data 3 Original and uncropped gels and blots.

Figure 1

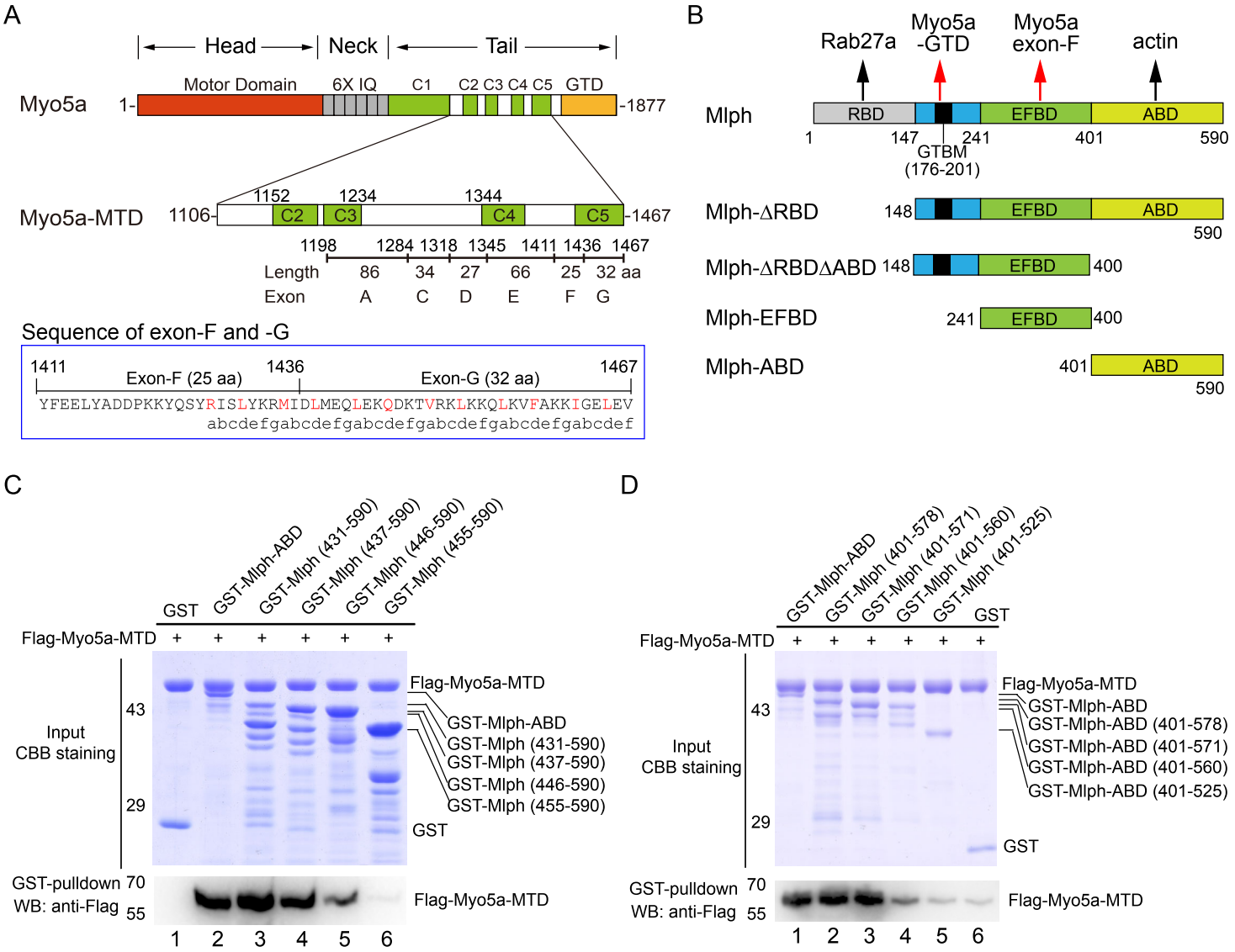
A
Head
Neck
Tail
Myo5a
1-
Motor Domain
6X IQ
C1
C2 C3 C4 C5
GTD
-1877
Myo5a-MTD
1106-
1152
1234
1344
C2
C3
C4
C5
-1467
1198
1284 1318
1345
1411 1436
1467
Length
86
34
27
66
25
32 aa
Exon
A
C
D
E
F
G
Sequence of exon-F and -G
1411
Exon-F (25 aa)
1436
Exon-G (32 aa)
1467
YFEELYADDPKKYQSYRISLYKRMIDLMEQLEKQDKTVRKLKKQLKVFAKKIGELEV
abcdefgabcdefgabcdefgabcdefgabcdefgabcdef
B
Rab27a
Myo5a -GTD
Myo5a exon-F
actin
Mlph
RBD
EFBD
ABD
1
147
241
401
590
GTBM (176-201)
Mlph-ΔRBD
148
EFBD
ABD
590
Mlph-ΔRBDΔABD
148
EFBD
400
Mlph-EFBD
241
EFBD
400
Mlph-ABD
401
ABD
590
C
GST
GST-Mlph-ABD
GST-Mlph (431-590)
GST-Mlph (437-590)
GST-Mlph (446-590)
GST-Mlph (455-590)
Flag-Myo5a-MTD
+ + + + + +
Input
CBB staining
43
29
Flag-Myo5a-MTD
GST-Mlph-ABD
GST-Mlph (431-590)
GST-Mlph (437-590)
GST-Mlph (446-590)
GST-Mlph (455-590)
GST
GST-pulldown
WB: anti-Flag
70
55
Flag-Myo5a-MTD
1 2 3 4 5 6
D
GST-Mlph-ABD
GST-Mlph (401-578)
GST-Mlph (401-571)
GST-Mlph (401-560)
GST-Mlph (401-525)
GST
Flag-Myo5a-MTD
+ + + + + +
Input
CBB staining
43
29
Flag-Myo5a-MTD
GST-Mlph-ABD
GST-Mlph-ABD (401-578)
GST-Mlph-ABD (401-571)
GST-Mlph-ABD (401-560)
GST-Mlph-ABD (401-525)
GST
GST-pulldown
WB: anti-Flag
70
55
Flag-Myo5a-MTD
1 2 3 4 5 6

Figure 2

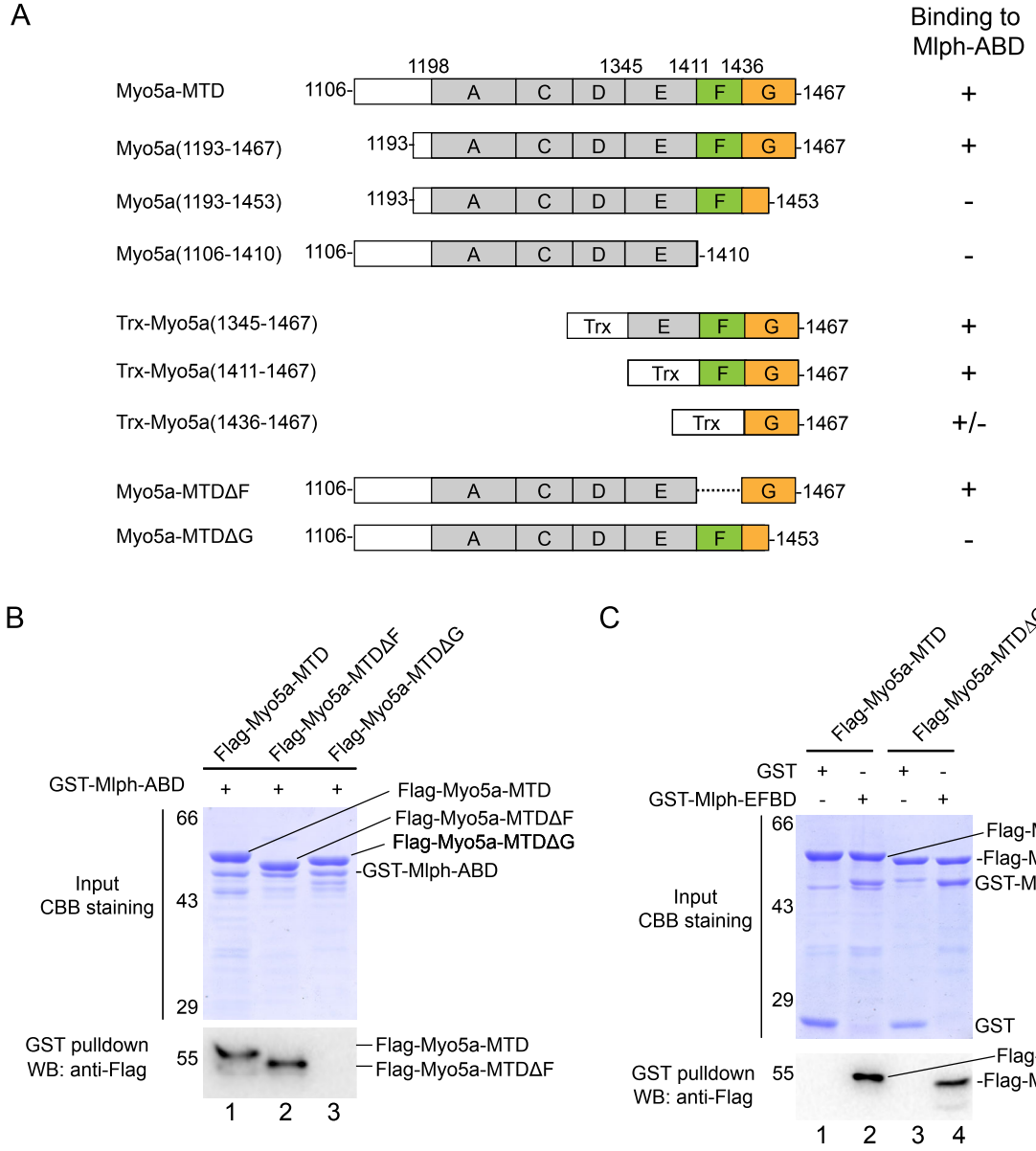
A
Binding to Mlph-ABD
1198
1345
1411
1436
Myo5a-MTD
1106-
A
C
D
E
F
G
-1467
+
Myo5a(1193-1467)
1193-
-1467
+
Myo5a(1193-1453)
1193-
-1453
-
Myo5a(1106-1410)
1106-
-1410
-
Trx-Myo5a(1345-1467)
Trx
-1467
+
Trx-Myo5a(1411-1467)
-1467
+
Trx-Myo5a(1436-1467)
-1467
+/-
Myo5a-MTDΔF
1106-
-1467
+
Myo5a-MTDΔG
1106-
-1453
-
B
Flag-Myo5a-MTD
Flag-Myo5a-MTDΔF
Flag-Myo5a-MTDΔG
GST-Mlph-ABD
+
+
+
Flag-Myo5a-MTD
Flag-Myo5a-MTDΔF
Flag-Myo5a-MTDΔG
-GST-Mlph-ABD
Input
CBB staining
66
43
29
GST pulldown
WB: anti-Flag
55
Flag-Myo5a-MTD
Flag-Myo5a-MTDΔF
1
2
3
C
Flag-Myo5a-MTD
Flag-Myo5a-MTDΔG
GST
+
-
+
-
GST-Mlph-EFBD
-
+
-
+
Flag-Myo5a-MTD
-Flag-Myo5a-MTDΔG
GST-Mlph-EFBD
Input
CBB staining
66
43
29
GST
GST pulldown
WB: anti-Flag
55
Flag-Myo5a-MTD
-Flag-Myo5a-MTDΔG
1
2
3
4

Figure 3

A

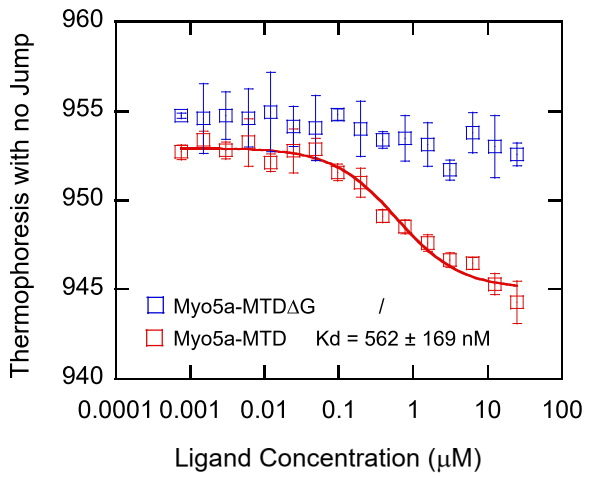

B

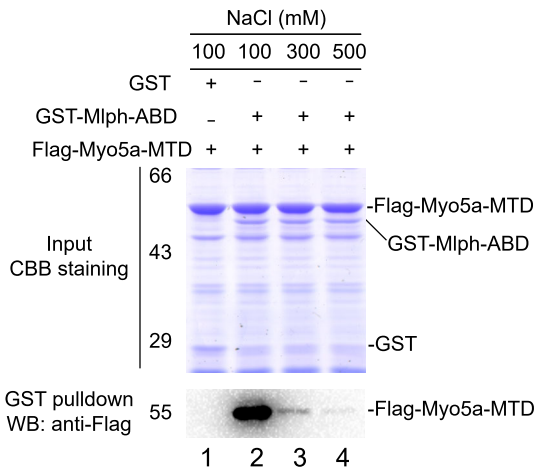

C

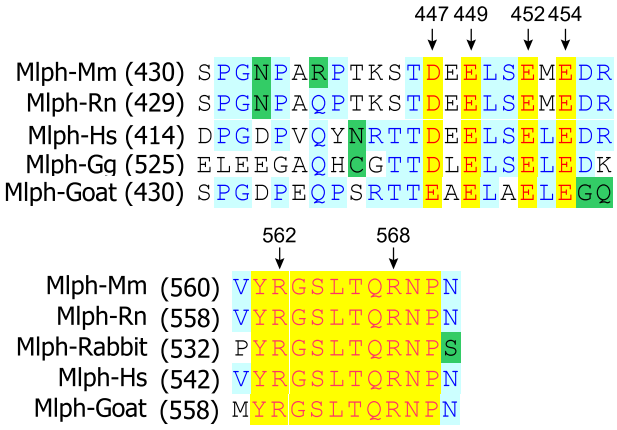

D

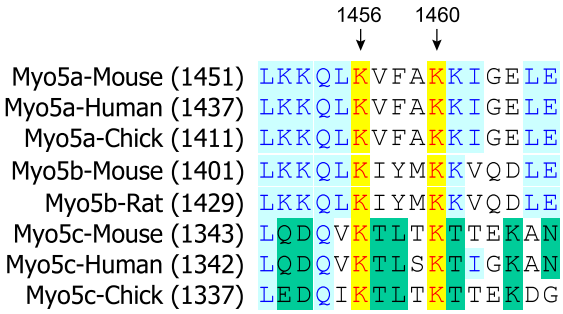

E

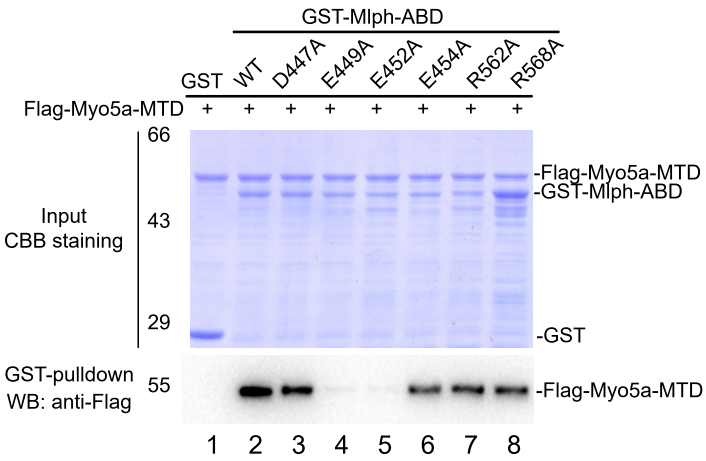

F

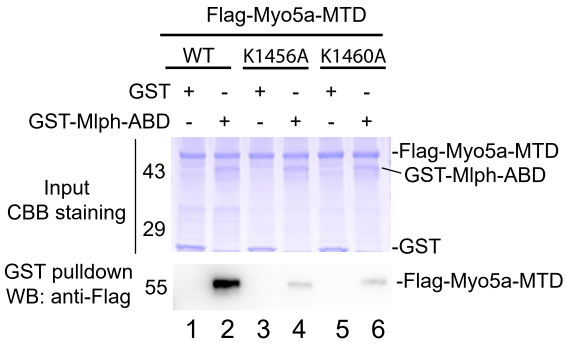

Figure 4

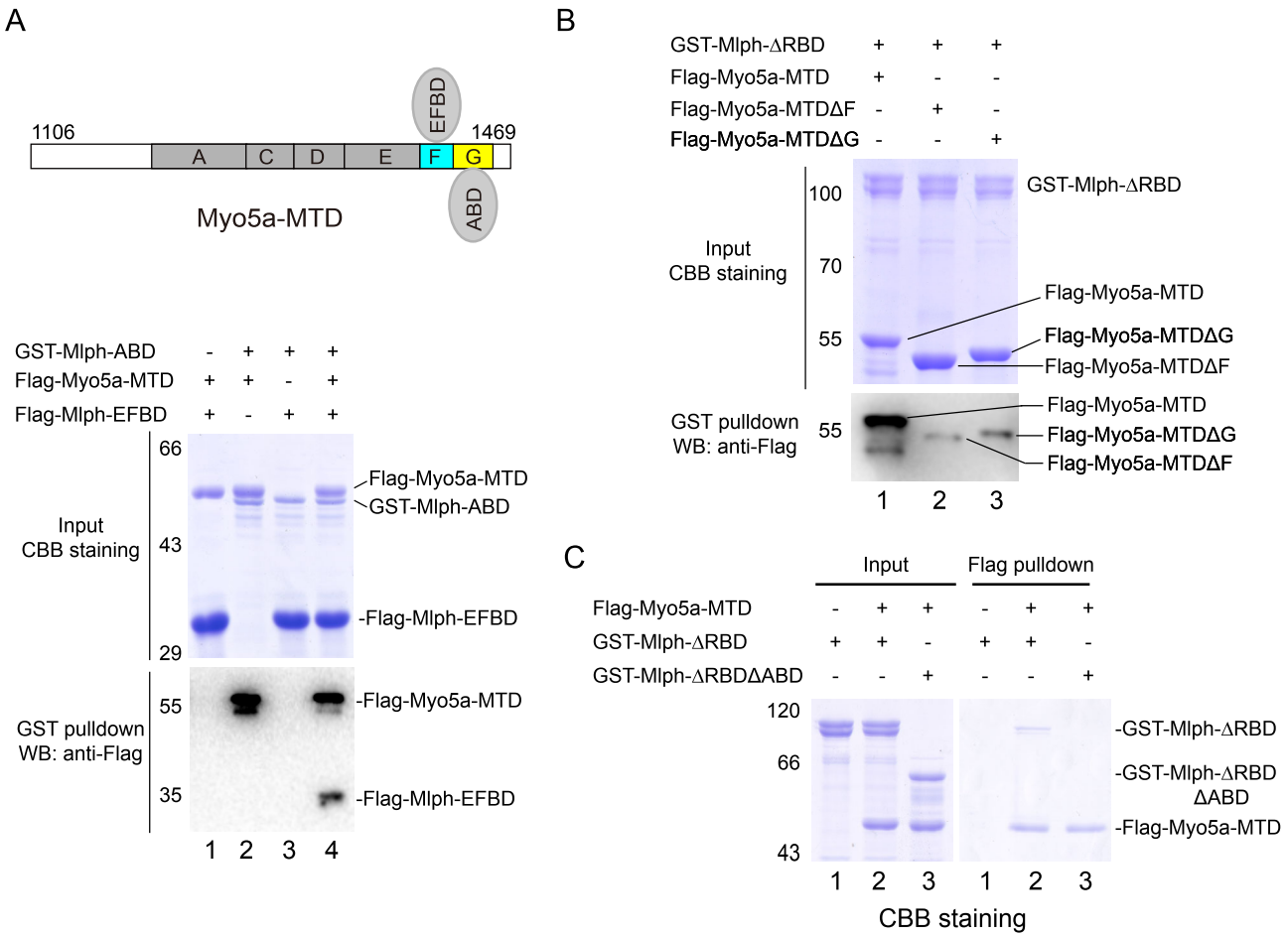
A
1106
1469
A
C
D
E
F
G
EFBD
ABD
Myo5a-MTD
GST-Mlph-ABD - + + +
Flag-Myo5a-MTD + + - +
Flag-Mlph-EFBD + - + +
Input
CBB staining
66
43
29
Flag-Myo5a-MTD
GST-Mlph-ABD
-Flag-Mlph-EFBD
GST pulldown
WB: anti-Flag
55
35
-Flag-Myo5a-MTD
-Flag-Mlph-EFBD
1 2 3 4
B
GST-Mlph-ΔRBD + + +
Flag-Myo5a-MTD + - -
Flag-Myo5a-MTDΔF - + -
Flag-Myo5a-MTDΔG - - +
Input
CBB staining
100
70
55
GST-Mlph-ΔRBD
Flag-Myo5a-MTD
Flag-Myo5a-MTDΔG
Flag-Myo5a-MTDΔF
GST pulldown
WB: anti-Flag
55
Flag-Myo5a-MTD
Flag-Myo5a-MTDΔG
Flag-Myo5a-MTDΔF
1 2 3
C
Input
Flag pulldown
Flag-Myo5a-MTD - + + - + +
GST-Mlph-ΔRBD + + - + + -
GST-Mlph-ΔRBDΔABD - - + - - +
120
66
43
-GST-Mlph-ΔRBD
-GST-Mlph-ΔRBD
ΔABD
-Flag-Myo5a-MTD
1 2 3 1 2 3
CBB staining

Figure 5

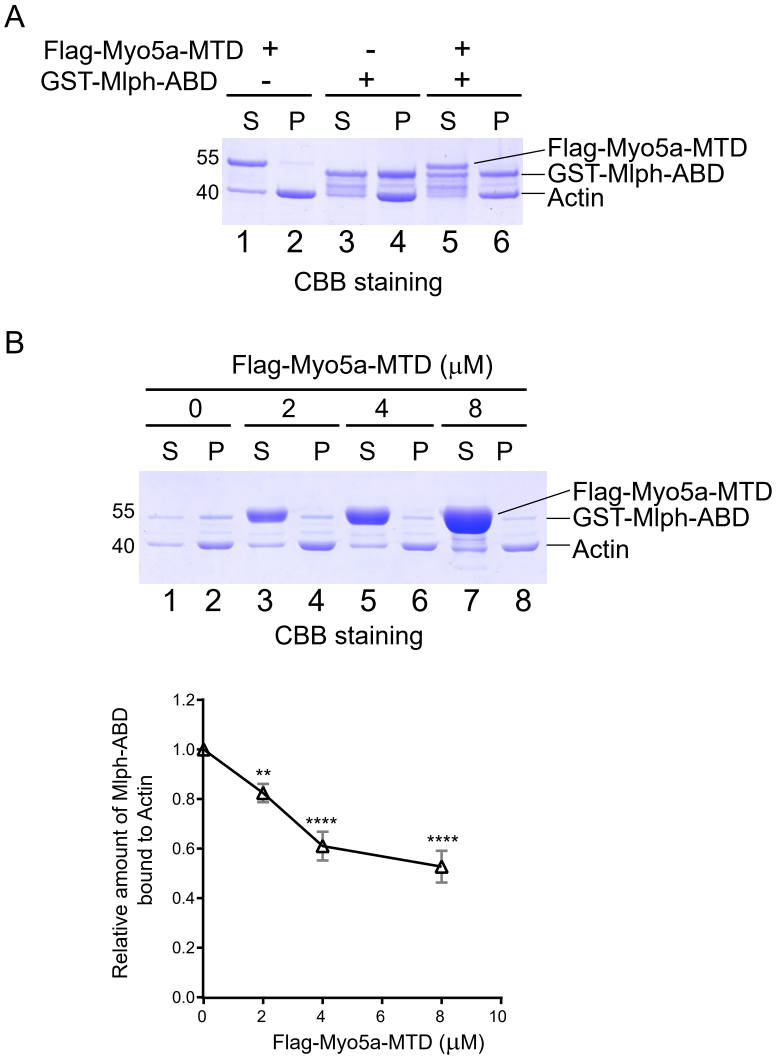
A
Flag-Myo5a-MTD + - +
GST-Mlph-ABD - + +
S P S P S P
55
40
Flag-Myo5a-MTD
GST-Mlph-ABD
Actin
1 2 3 4 5 6
CBB staining
B
Flag-Myo5a-MTD (μM)
0 2 4 8
S P S P S P S P
55
40
Flag-Myo5a-MTD
GST-Mlph-ABD
Actin
1 2 3 4 5 6 7 8
CBB staining
Relative amount of Mlph-ABD bound to Actin
1.2
1.0
0.8
0.6
0.4
0.2
0.0
**
****
****
0 2 4 6 8 10
Flag-Myo5a-MTD (μM)

Figure 6

A

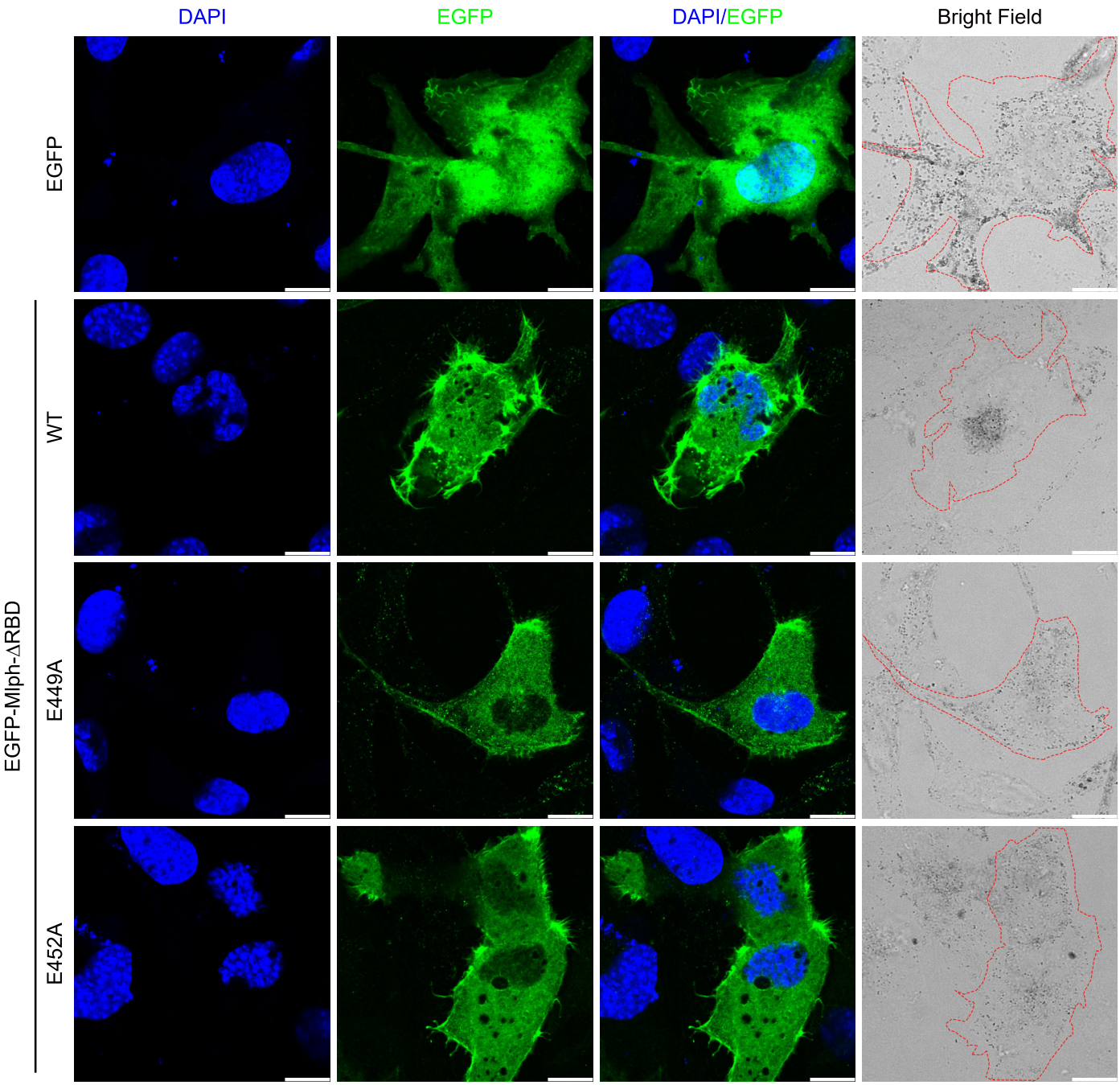
DAPI
EGFP
DAPI/EGFP
Bright Field
EGFP
EGFP-Mlph-ΔRBD
WT
E449A
E452A

B

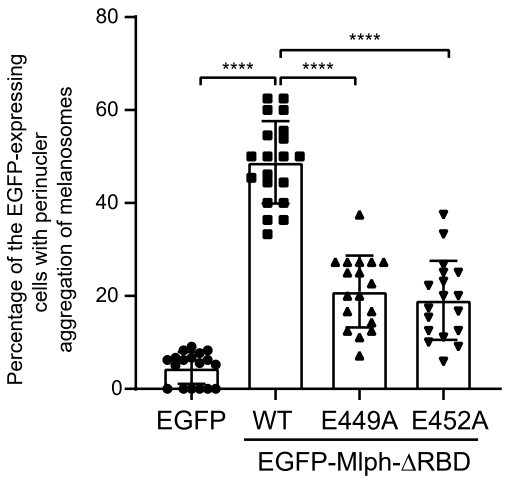
Percentage of the EGFP-expressing cells with perinucler aggregation of melanosomes
80
60
40
20
0
****
****
****
EGFP
WT
E449A
E452A
EGFP-Mlph-ΔRBD

C

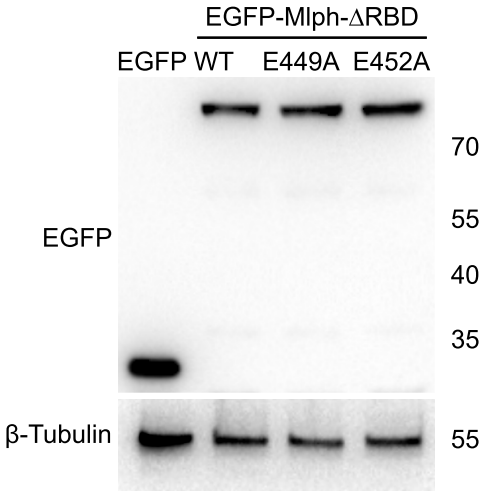
EGFP-Mlph-ΔRBD
EGFP
WT
E449A
E452A
EGFP
β-Tubulin
70
55
40
35
55

Figure 7

A

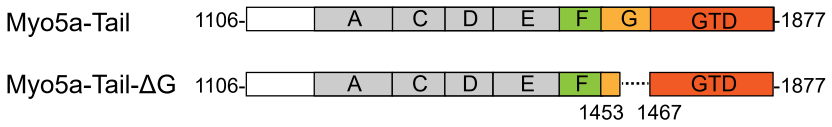

B

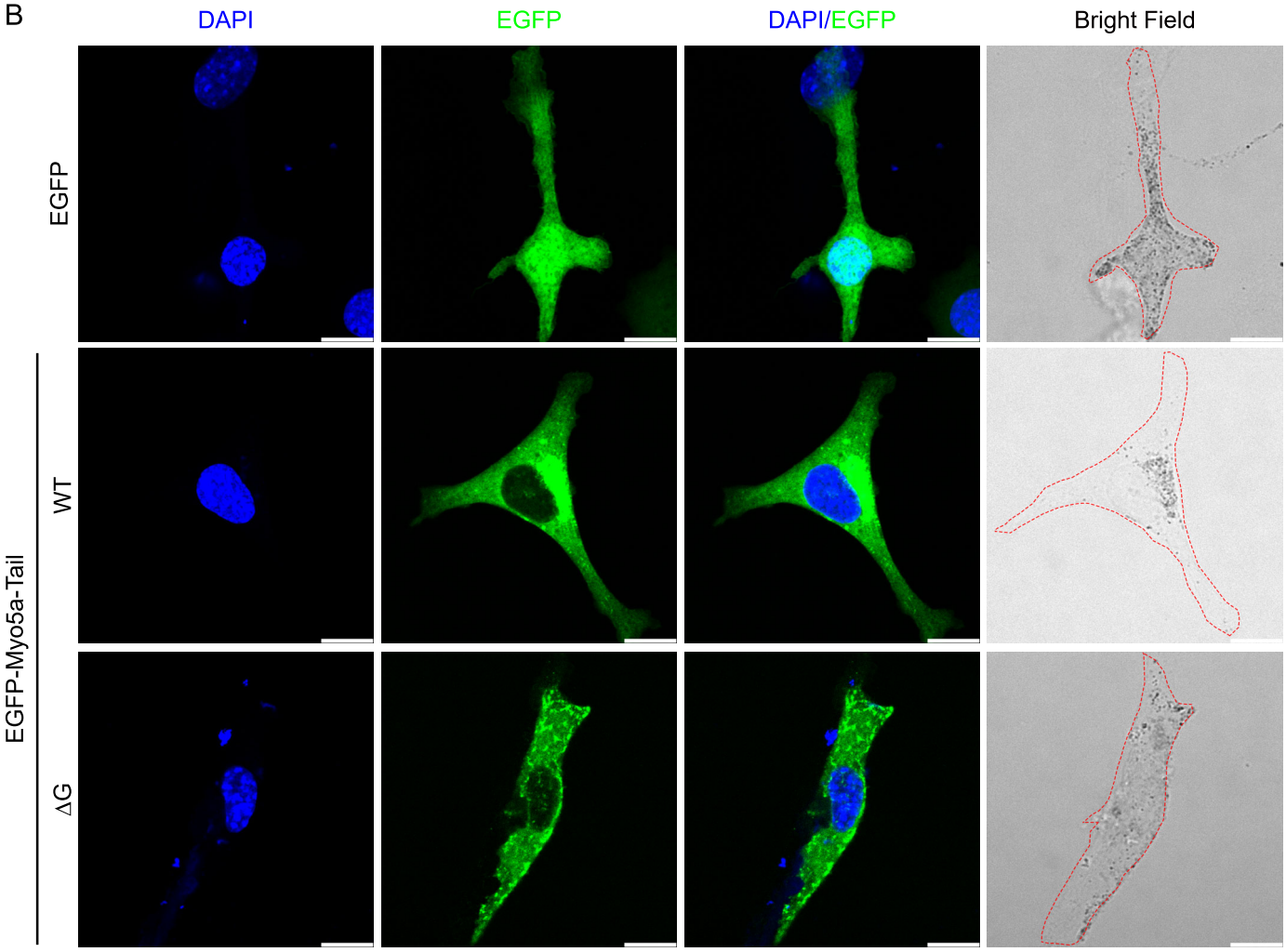

C

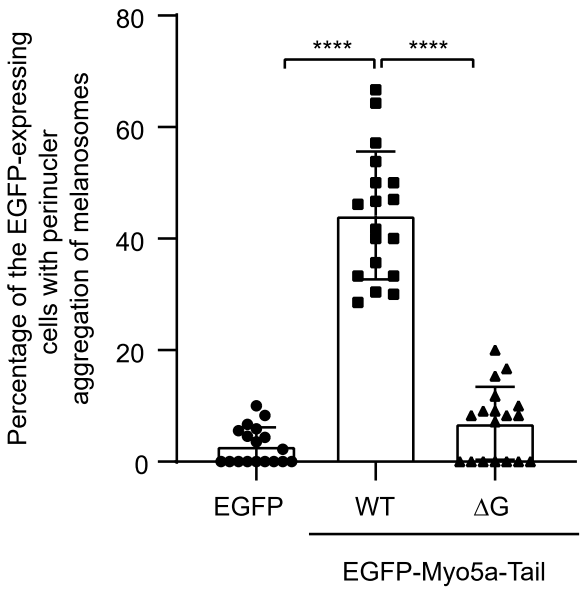

D

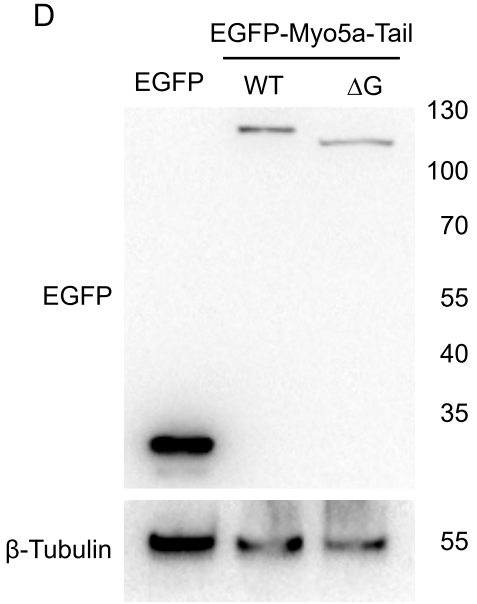

Figure 8

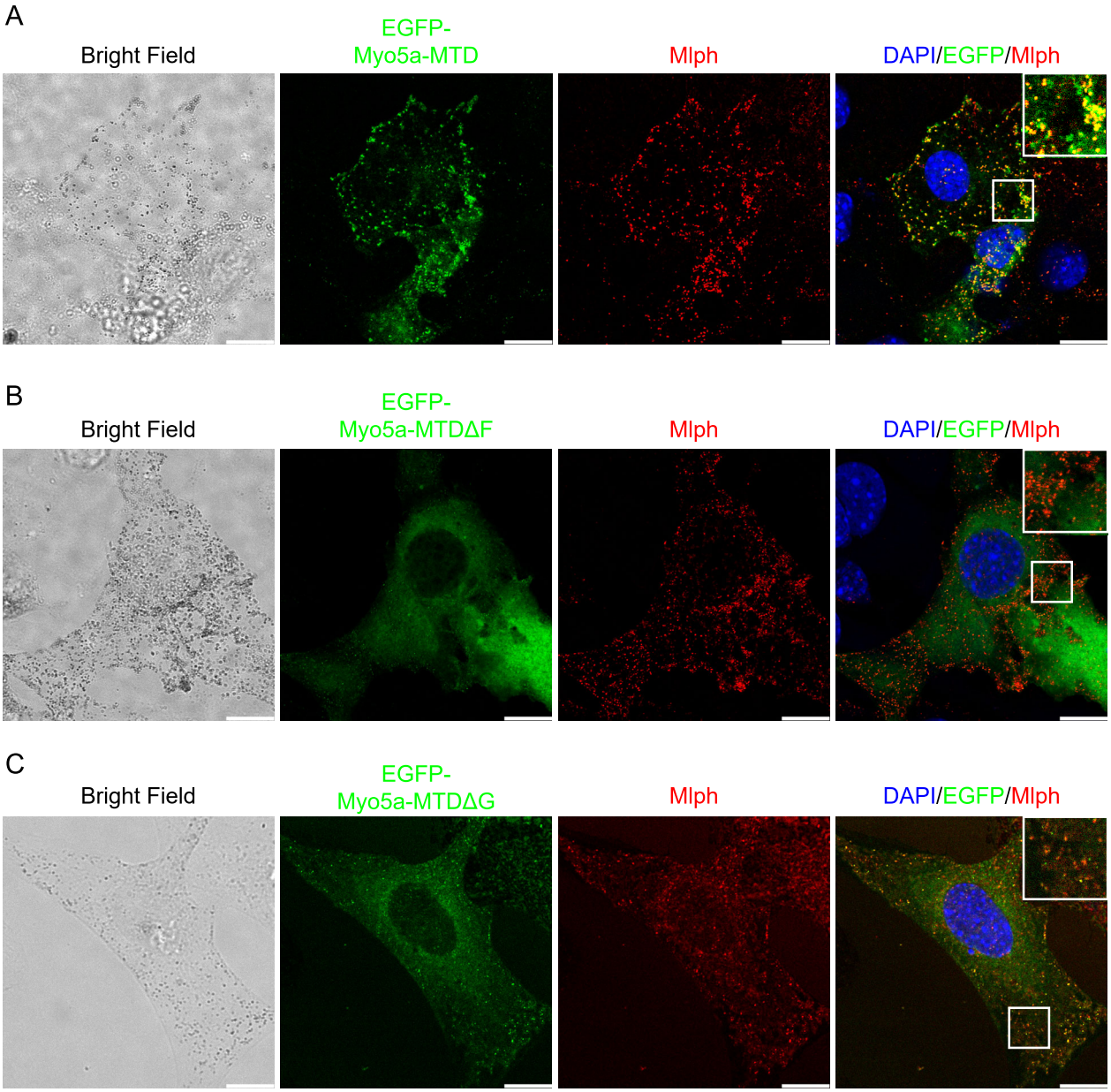
A
Bright Field
EGFP-
Myo5a-MTD
Mlph
DAPI/EGFP/Mlph
B
Bright Field
EGFP-
Myo5a-MTDΔF
Mlph
DAPI/EGFP/Mlph
C
Bright Field
EGFP-
Myo5a-MTDΔG
Mlph
DAPI/EGFP/Mlph

Figure 9

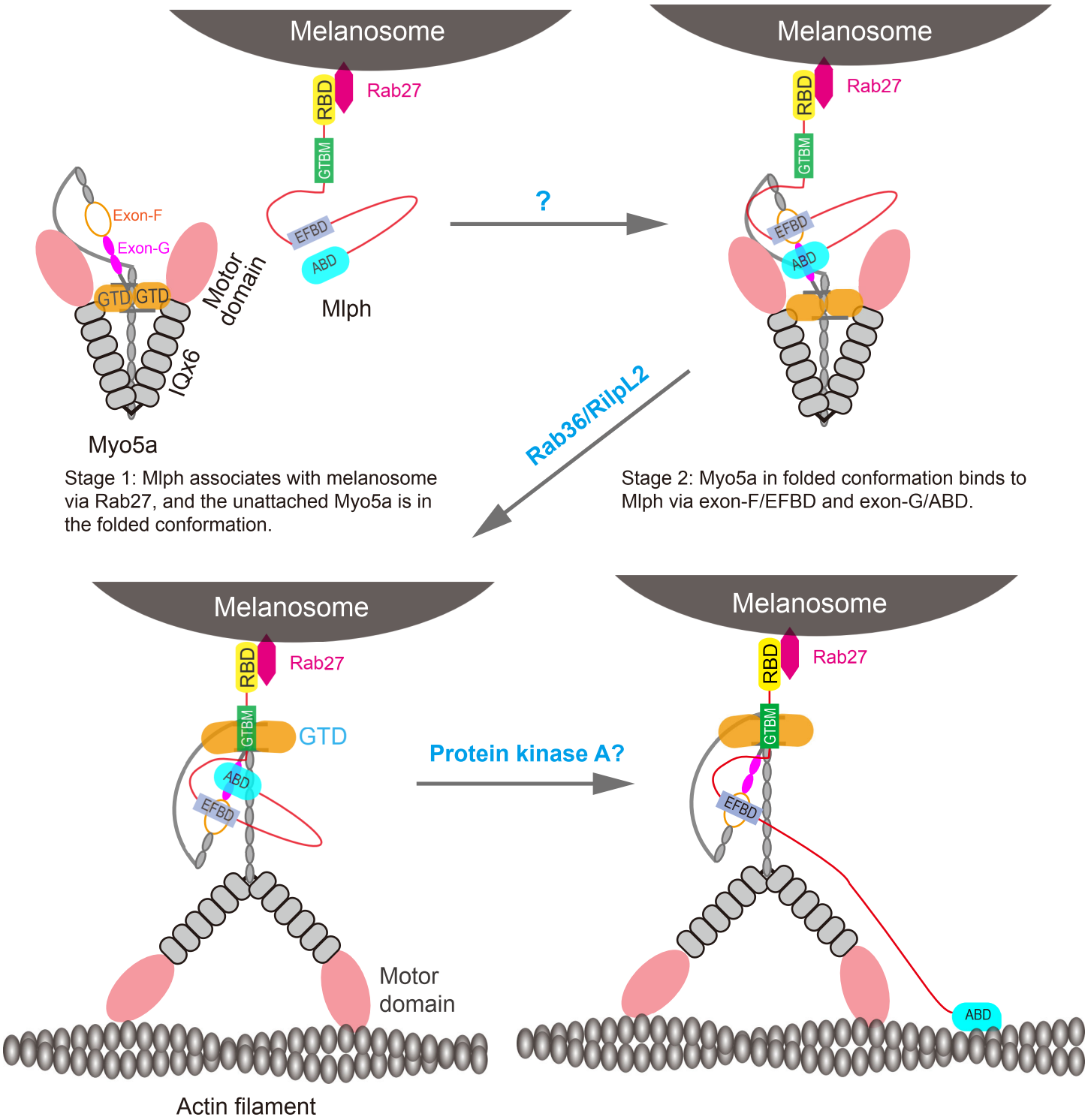

Stage 1: Mlph associates with melanosome via Rab27, and the unattached Myo5a is in the folded conformation.

Stage 2: Myo5a in folded conformation binds to Mlph via exon-F/EFBD and exon-G/ABD.

Stage 3: Mlph-GTBM binds to the GTD and induces Myo5a to form the extended conformation.

Stage 4: Mlph-ABD dissociates from exon-G, and then binds to actin filament, enhancing the processibility of Myo5a.

Figure 2-figure supplement

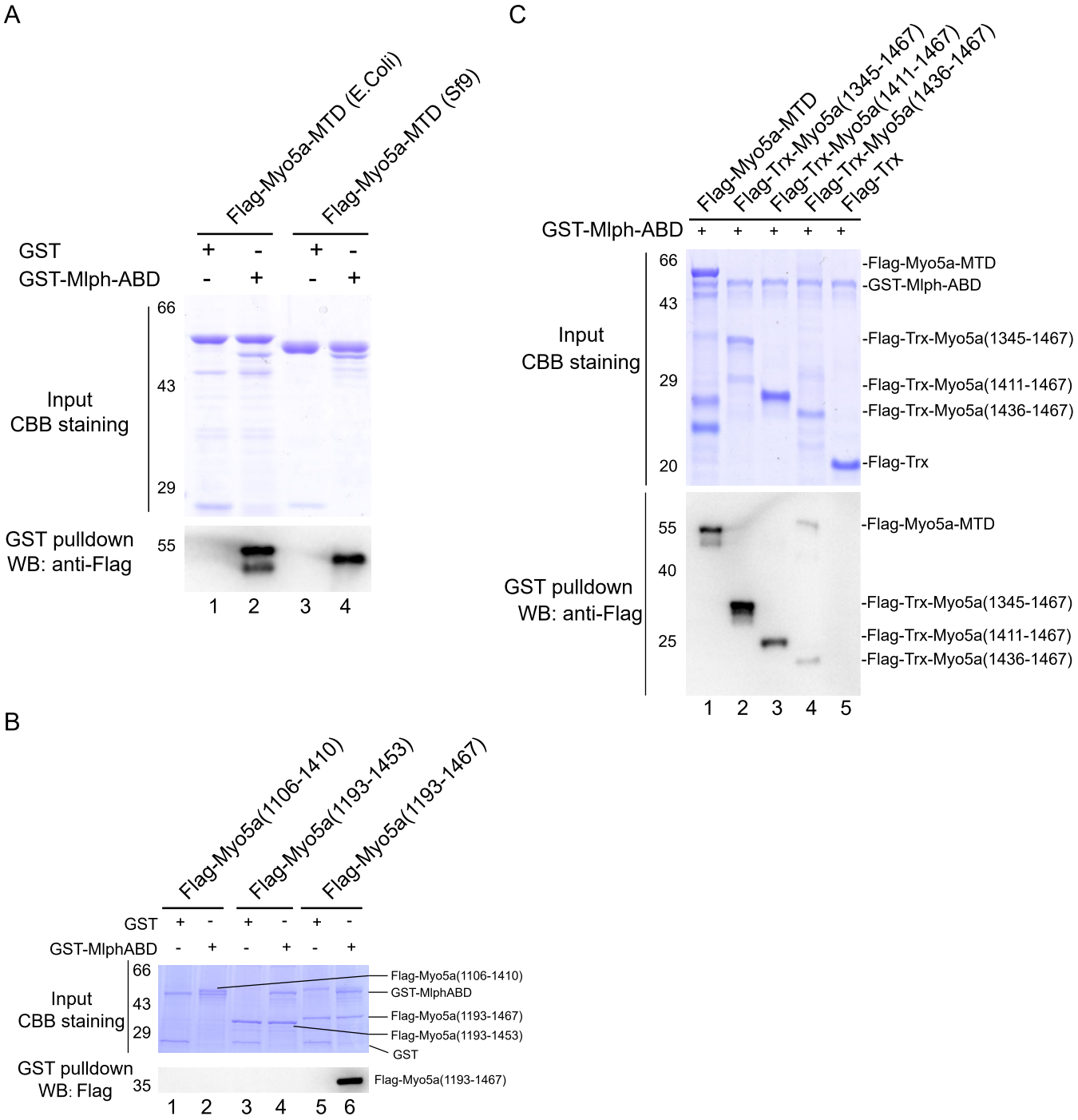

Figure 6-figure supplement

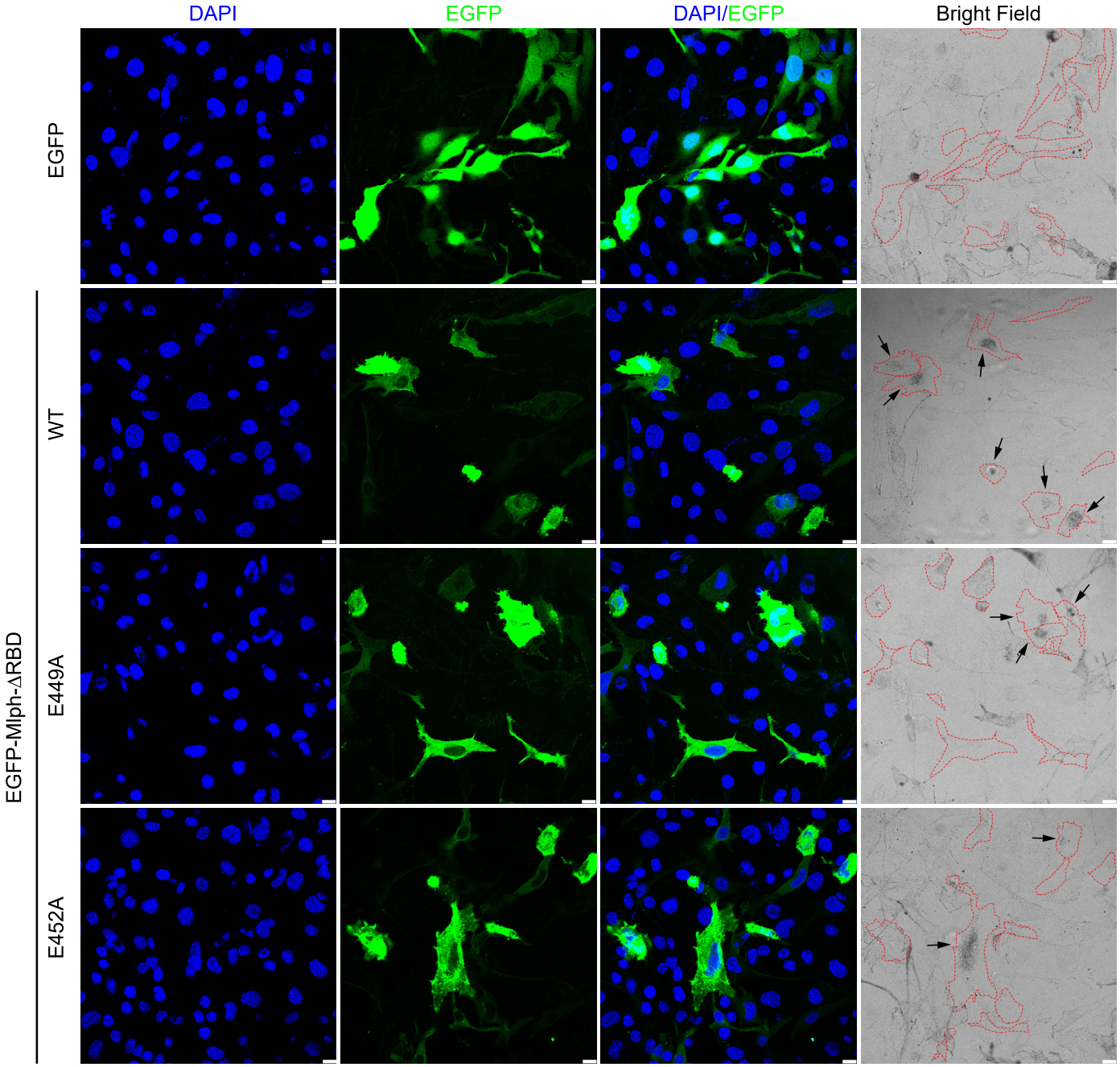
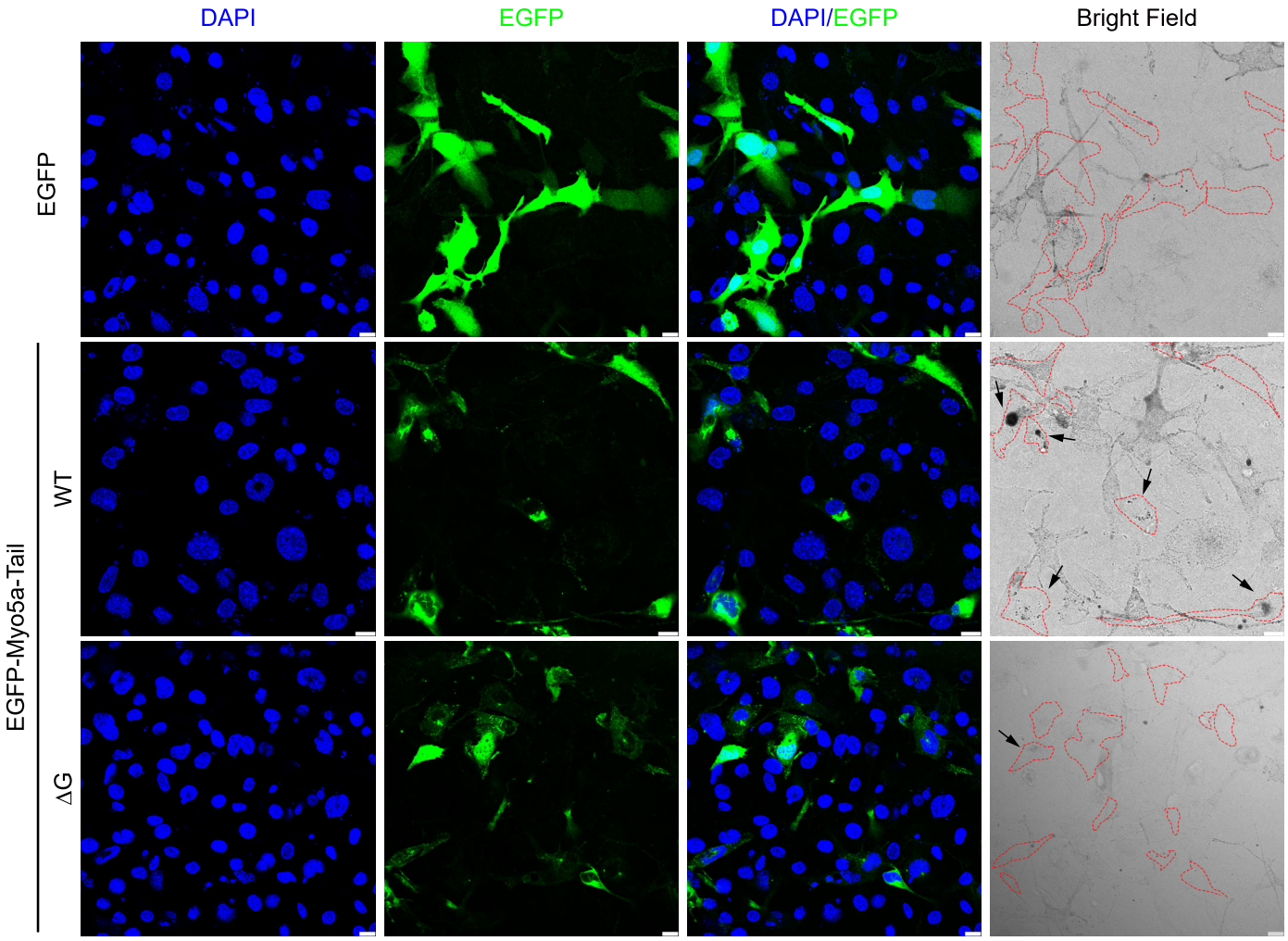
Figure 7-figure supplement